




Biogeography, Assembly Patterns, Driving Factors, and Interactions of Archaeal Community in Mangrove Sediments

Zhi-Feng Zhang,^{a,b} Jie Pan,^a Yue-Ping Pan,^a  Meng Li^a

^aShenzhen Key Laboratory of Marine Microbiome Engineering, Institute for Advanced Study, Shenzhen University, Shenzhen, China

^bKey Laboratory of Optoelectronic Devices and Systems of Ministry of Education and Guangdong Province, College of Optoelectronic Engineering, Shenzhen University, Shenzhen, China

ABSTRACT Archaea are a major part of Earth's life. They are believed to play important roles in nutrient biogeochemical cycling in the mangrove. However, only a few studies on the archaeal community in mangroves have been reported. In particular, the assembly processes and interaction patterns that impact the archaeal communities in mangroves have not been investigated to date. Here, the biogeography, assembly patterns, and driving factors of archaeal communities in seven representative mangroves across southeastern China were systematically analyzed. The analysis revealed that the archaeal community is more diverse in surface sediments than in subsurface sediments, and more diverse in mangroves at low latitudes than at high latitudes, with *Woesearchaeota* and *Bathyarchaeota* as the most diverse and most abundant phyla, respectively. Beta nearest-taxon index analysis suggested a determinant role of homogeneous selection on the overall archaeon community in all mangroves and in each individual mangrove. In addition, the conditionally rare taxon community was strongly shaped by homogeneous selection, while stochastic processes shaped the dominant taxon and always-rare taxon communities. Further, a moderate effect of environmental selection on the archaeal community was noted, with the smallest effect on the always-rare taxon community. Mangrove location, mean annual temperature, and salinity were the major factors that greatly affected the community composition. Finally, network analysis revealed comprehensive cooccurrence relationships in the archaeal community, with a crucial role of *Bathyarchaeota*. This study expands the understanding of the biogeography, assembly patterns, driving factors, and cooccurrence relationships of the mangrove archaeal community and inspires functional exploration of archaeal resources in mangrove sediments.

IMPORTANCE As a key microbial community component with important ecological roles, archaea merit the attention of biologists and ecologists. The mechanisms controlling microbial community diversity, composition, and biogeography are central to microbial ecology but poorly understood. Mangroves are located at the land-ocean interface and are an ideal environment for examining the above questions. We here provided the first-ever overview of archaeal community structure and biogeography in mangroves located along an over-9,000-km coastline of southeastern China. We observed that archaeal diversity in low-latitude mangroves was higher than that in high-latitude mangroves. Furthermore, our data indicated that homogeneous selection strongly controlled the assembly of the overall and conditionally rare taxon communities in mangrove sediments, while the dominant taxon and always-rare taxon communities were mainly controlled by dispersal limitation.

KEYWORDS archaeal community, neutral community model, beta nearest-taxon index, homogeneous selection, cooccurrence network, mangrove sediment

Citation Zhang Z-F, Pan J, Pan Y-P, Li M. 2021. Biogeography, assembly patterns, driving factors, and interactions of archaeal community in mangrove sediments. *mSystems* 6:e01381-20. <https://doi.org/10.1128/mSystems.01381-20>.

Editor Jack A. Gilbert, University of California San Diego

Copyright © 2021 Zhang et al. This is an open-access article distributed under the terms of the [Creative Commons Attribution 4.0 International license](https://creativecommons.org/licenses/by/4.0/).

Address correspondence to Meng Li, limeng848@szu.edu.cn.

Received 31 December 2020

Accepted 20 May 2021

Published 15 June 2021

Mangrove wetlands are widely distributed along the coast in tropical and subtropical regions. They play important ecological roles, such as protecting the coastal area and providing food and shelter for fish and shellfish (1, 2). Although they cover less than 1% of the tropical surface area, they account for 11% of the total input of terrestrial carbon into the ocean and 10% of the terrestrial dissolved organic carbon exported to the ocean, making them a “blue carbon sink” (1, 3, 4). Because of specific ecological features, such as high nutrient concentration and high salinity, low oxygen and low pH, strong redox potential, and vertical sedimentary physicochemical gradients, mangrove ecosystems may harbor numerous adapted organisms (5, 6). Archaea are key components of the microbial community in mangroves, with relative proportions up to 20.8 to 41.3% (7) in the prokaryotic community. They are supposed to have abundant and diverse metabolic pathways (8), such as ammonia oxidation (9, 10), degradation of organic matter (10–12), methane metabolism (13, 14), and sulfate reduction (15, 16), indicating key roles of archaea in driving complex nutrient and biogeochemical cycling in mangrove sediments.

While archaea may have important ecological functions in mangrove and are thus immensely interesting to biologists and ecologists, there is a dearth of studies on archaeal community assembly in mangroves. Yan et al. (17) were the first to reveal a predominance of *Crenarchaeota* and *Euryarchaeota* archaea in mangrove sediments using the analysis of 16S rRNA gene clones. By comparing archaeal communities in pristine and oil-polluted mangroves, Bhattacharyya et al. (18) demonstrated a clear community shift in response to environmental conditions. Recent studies have mainly focused on the effect of spatial, temporal, and environmental variables on the archaeal community. For instance, seasonality, sediment depth, and pH have important effects on the archaeal community (7, 19–22), and total organic carbon (TOC) and nitric oxide are significantly correlated with the abundance of *Bathyarchaeota* (22). However, most of the above studies of the archaeal community were focused on individual mangroves and seldom provide an integrative view of the influence patterns of spatial and environmental parameters on a large geographical scale.

Understanding the forces that mold the community composition structure is a major goal of microbial ecology (23). Microbial community assembly and the mechanisms shaping the community diversity, distribution, and biogeography are central but poorly understood topics of aquatic microbial ecology (23–26). Community assembly is simultaneously shaped by deterministic and stochastic factors (23, 25, 26). The former include selection imposed by abiotic (environmental factors) and biotic (species interactions) factors, and the latter include unpredictable ecological events, such as birth, death, immigration, speciation, and limited dispersal (23, 25). As fluctuating ecosystems at the land-ocean interface with important ecological roles, mangroves provide a unique environment wherein to examine the community assembly theories. Although there are several studies exploring microbial community composition and the influencing factors in mangroves, few have tried to dissect the relative importance of stochastic and deterministic processes therein. Zhang et al. (13) reported a relatively more important role of the deterministic process rather than of the stochastic process in shaping the entire prokaryotic community assembly in mangroves. However, the knowledge of archaeal community assembly in mangroves is still limited.

According to several studies, some taxa with low relative abundance (i.e., rare taxa) are in fact metabolically active and may act as keystones that regulate the functions of aquatic ecosystems. Hence, the microbes of the “rare biosphere” have important roles in the metabolic and ecological functions of aquatic habitats (26–28). For example, rare archaea are supposed to have ecological functions, such as acetate metabolism (29), carbon cycling (30), and methanogenesis (31). Another interesting component is the taxa which are usually rare but occasionally become more prominent under optimal conditions, namely, the conditionally rare taxa (26, 28, 32). Conditionally rare taxa can explain large temporal shifts of microbial structure (29, 33). However, the knowledge of many ecosystems, including mangrove wetlands, is mostly based on dominant or

entire communities, with the roles of always-rare taxa and conditionally rare taxa rarely accounted for (29). Consequently, to explore the assembly patterns, biogeography, and potential controlling factors of the “rare biosphere” in mangrove sediments, the archaeal community in the current study was separated into dominant taxa, conditionally rare taxa, and always-rare taxa.

Accordingly, in the current study, we aimed to shed light on the processes that govern the archaeal community assembly in mangroves on a large scale. Large-scale sampling could provide data for estimating natural distributions and building species distribution models (34). To do this, we characterized the archaeal communities in 127 samples from seven representative mangroves along the Southeast China coast (see Data Set S1, sheet 1, in the supplemental material). We first explored the diversity, biogeography, and composition of archaeal communities. Then, we quantified the community assembly processes using neutral community model (NCM) fitting and beta nearest-taxon index (β NTI). In addition, we determined the selection by environmental factors using variation partition analysis (VPA) and distance-based redundancy analysis (db-RDA). Finally, we explored species interactions within the archaeal community based on cooccurrence correlation. The analysis allowed us to address the following questions. (i) Do all, dominant, conditionally rare, and always-rare archaeal taxa exhibit similar or different biogeography and community compositions? (ii) Do all, dominant, conditionally rare, and always-rare archaeal taxa assemble via different community assembly processes? (iii) How much do the deterministic and stochastic processes control the community assembly? (iv) Which environmental factor has the greatest effect on archaeal community composition?

RESULTS

Composition and diversity of archaeal community in mangrove sediments. In the study, seven representative mangroves (DZG, FT, SK, XMD, YLW, ZJ, and ZJK) along the Southeast China coast were sampled (127 samples; see Data Set S1, sheet 1, in the supplemental material). Then, 16S rRNA genes were sequenced from samples from different sediment depths. After quality filtering and chimeric sequence removal, 4,926,673 high-quality sequences were clustered into 23,481 operational taxonomic units (OTUs), of which 15,514 were assigned as *Archaea*. After bacterial OTU removal, the archaeal OTU table was used for the ensuing analyses. Between 19,206 and 43,750 archaeal sequences were detected in each sample, with an average of 33,963 sequences per sample (Data Set S1, sheet 2). Rarefaction curve analysis indicated that most samples reached saturation (Fig. S1a), and archaeal OTU accumulation curves for different mangroves were nearly asymptotic (Fig. S1b). Comparison of α -diversity indices revealed higher archaeal richness in the 0- to 10-cm depth layer than that in the 20- to 30-cm layer in terms of OTU richness ($P < 0.05$), while none of the other indices were significantly different among the different depth layers (Fig. S2).

Although *Woesearchaeota* exhibited the highest OTU richness (58.9% of OTUs, 12.8% of archaeal sequences), *Bathyarchaeota* was the most abundant archaeal phylum in most samples, accounting for 7.0% (SK6-2) to 72.3% (ZJ1-2) of archaeal sequences (Fig. 1a and b; Data Set S1, sheet 2), with an overall sequence proportion of 39.8%. *Euryarchaeota* (8.8% of OTUs, 17.8% of sequences) and Asgard archaea (2.0% of OTUs, 8.7% of sequences) were also predominant in the mangrove archaeal community. The relative abundance of Asgard archaea and *Bathyarchaeota* in the 10- to 20-cm and 20- to 30-cm depth layers was significantly higher than that in the 0- to 10-cm depth layer ($P < 0.05$). The relative abundance of *Thaumarchaeota* and *Woesearchaeota* was significantly higher in the 0- to 10-cm depth layer than in the 10- to 20-cm and 20- to 30-cm depth layers ($P < 0.015$) (Fig. S3).

According to the criteria described in Materials and Methods, a high proportion of OTUs were identified as always-rare taxa (mean = 33.6%) and conditionally rare taxa (mean = 65.1%), but they accounted for only 0.7% and 31.0% of the average relative abundance in each sample, respectively. Conversely, a low proportion of OTUs

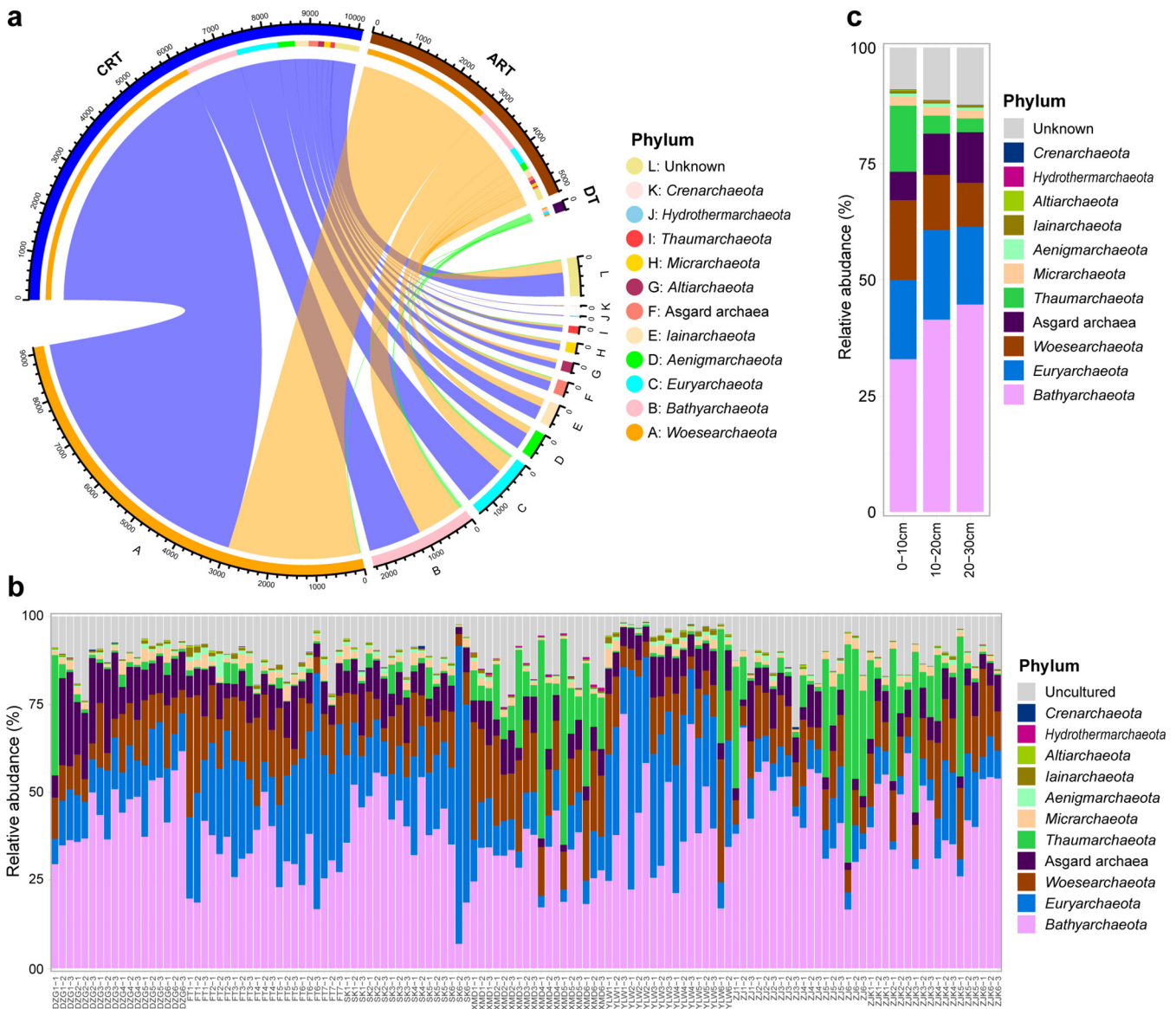


FIG 1 Taxonomic composition of the archaeal community. (a) Archaeal OTUs of dominant taxa (DT), conditionally rare taxa (CRT), and always-rare taxa (ART) at phylum level. The colors of the top half of the outer ring represent DT, CRT, and ART, respectively. The lower half of the outer ring is colored according to the phyla specified in the key. Line thickness corresponds to the numbers of OTUs in different groups. (b) Relative abundance of phyla in each sample. (c) Relative abundance of phyla in three depth layers.

(mean = 1.3%) were identified as dominant taxa and accounted for 68.3% of the average relative abundance in each sample (Fig. 1a; Data Set S1, sheet 2).

Comparison of the archaeal OTUs in the subsurface (10- to 30-cm) and surface (0- to 10-cm) sediments revealed a higher count of depleted OTUs (344 OTUs, 2.2% of archaeal OTUs) than enriched OTUs (308 OTUs, 1.9% of archaeal OTUs) in the subsurface sediment layers (Fig. 2a and b). Most of the enriched OTUs belonged to *Bathyarchaeota* (183 OTUs, 59.4% of enriched OTUs), *Euryarchaeota* (39 OTUs, 12.7% of enriched OTUs), *Woesearchaeota* (25 OTUs, 8.1% of enriched OTUs), Asgard archaea (21 OTUs, 6.8% of enriched OTUs), *Thaumarchaeota* (11 OTUs, 3.6% of enriched OTUs), and *Micrarchaeota* (6 OTUs, 2.0% of enriched OTUs). The depleted OTUs mainly belonged to *Woesearchaeota* (282 OTUs, 82.0% of depleted OTUs), *Euryarchaeota* (21 OTUs, 6.1% of depleted OTUs), Asgard archaea (14 OTUs, 4.1% of depleted OTUs), and *Thaumarchaeota* (6 OTUs, 1.7% of depleted OTUs). This suggested pronounced depletion of *Woesearchaeota* and enrichment of *Bathyarchaeota* in deeper sediments, which exhibited higher and lower relative

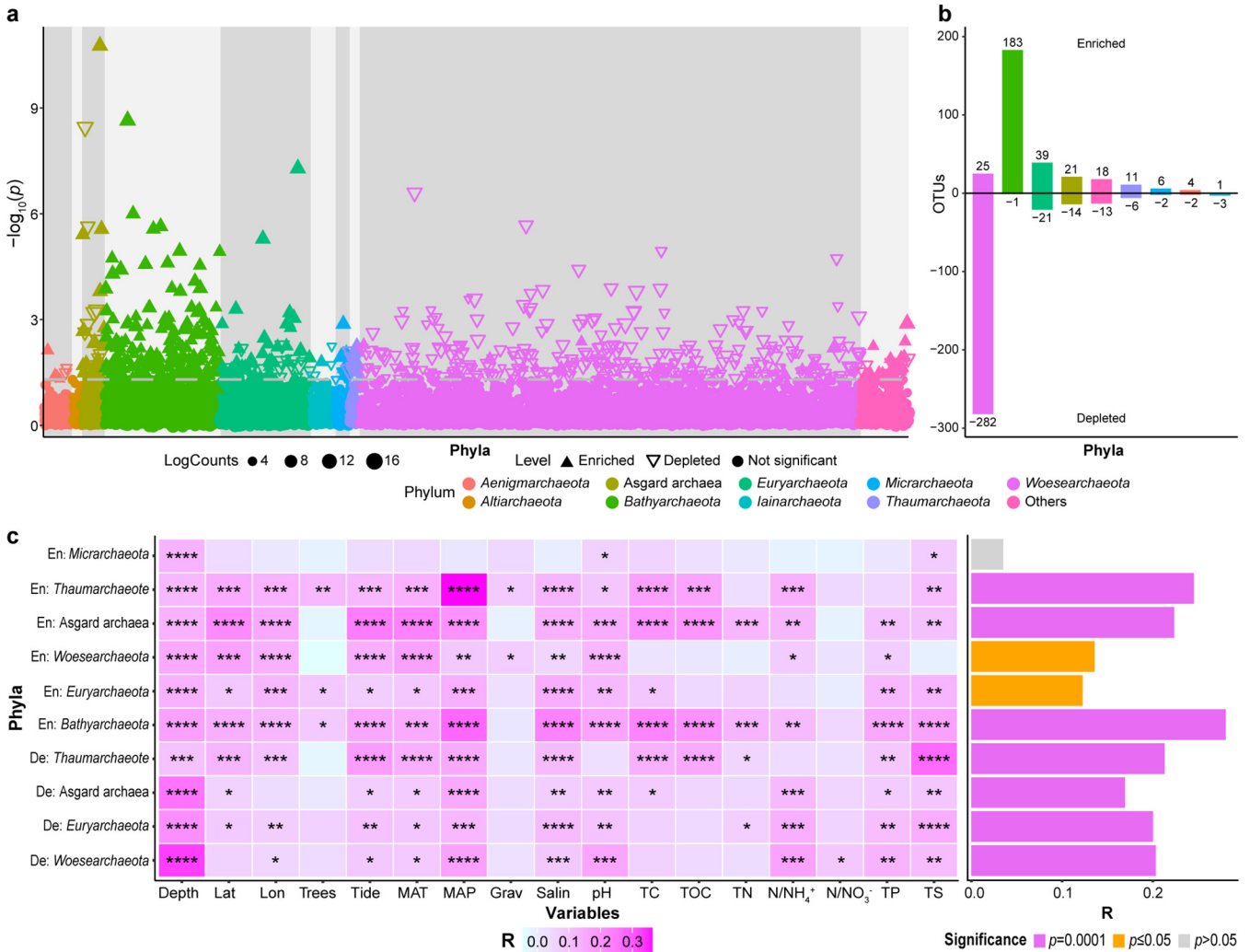


FIG 2 Comparison of OTUs' distribution between surface and subsurface mangrove sediments. (a) Comparison of OTU composition in the surface (0- to 10-cm) sediment samples and subsurface (10- to 30-cm) sediment samples in mangroves. Counts, total read number. Dashed line, 95% confidence level. Solid upward triangles, OTUs significantly enriched in subsurface sediments. Hollow downward triangles, OTUs significantly depleted in subsurface sediments. Solid points, OTUs with unchanged abundance in subsurface sediments compared with surface sediments. Triangle and point sizes are proportional to the abundance of that OTU. (b) Numbers of enriched and depleted OTUs in subsurface sediments compared with those in surface sediments at phylum level. (c) Mantel test for the effects of environmental variables on enriched and depleted phyla in subsurface sediments. Left, the effects of individual variables, denoted by the color gradient: *, $P \leq 0.05$; **, $P \leq 0.01$; ***, $P \leq 0.001$; ****, $P \leq 0.0001$. Right, the effects of all variables combined.

abundance in the 10- to 30-cm depth layers than in the 0- to 10-cm depth layer, respectively (Fig. S3). Depleted *Woesearchaeota* OTUs were significantly affected by depth, longitude, tidal height, mean annual temperature (MAT), mean annual precipitation (MAP), salinity, pH, ammonium nitrogen (N/NH₄⁺), nitrate nitrogen (N/NO₃⁻), total phosphorus (TP), and total sulfur (TS) (Mantel test, $P < 0.05$), and the correlation coefficient for all variables combined was 0.2030 (Mantel test, $P = 0.0001$) (Fig. 2c). In contrast, the enriched *Woesearchaeota* OTUs were further significantly affected by the latitude and gravel proportion, instead of N/NO₃⁻ and TS (Mantel test, $P < 0.05$), and the correlation with all variables combined was 0.1356 (Mantel test, $P = 0.0001$) (Fig. 2c). The enriched *Bathyarchaeota* OTUs were significantly influenced by almost all variables evaluated in the study, individually (Mantel test, $P < 0.05$) and combined (Mantel test, $R = 0.2800$, $P = 0.0001$) (Fig. 2c). Further, the remaining phyla with more than five depleted or enriched OTUs, except for the depleted *Micrarchaeota*, were significantly affected by all variables combined (Mantel test, $P < 0.05$) (Fig. 2c).

Archaeal community assembly patterns in mangrove ecosystems. The NCM fitted well the archaeal community assembly in all and individual mangroves ($R^2 > 0.6$)

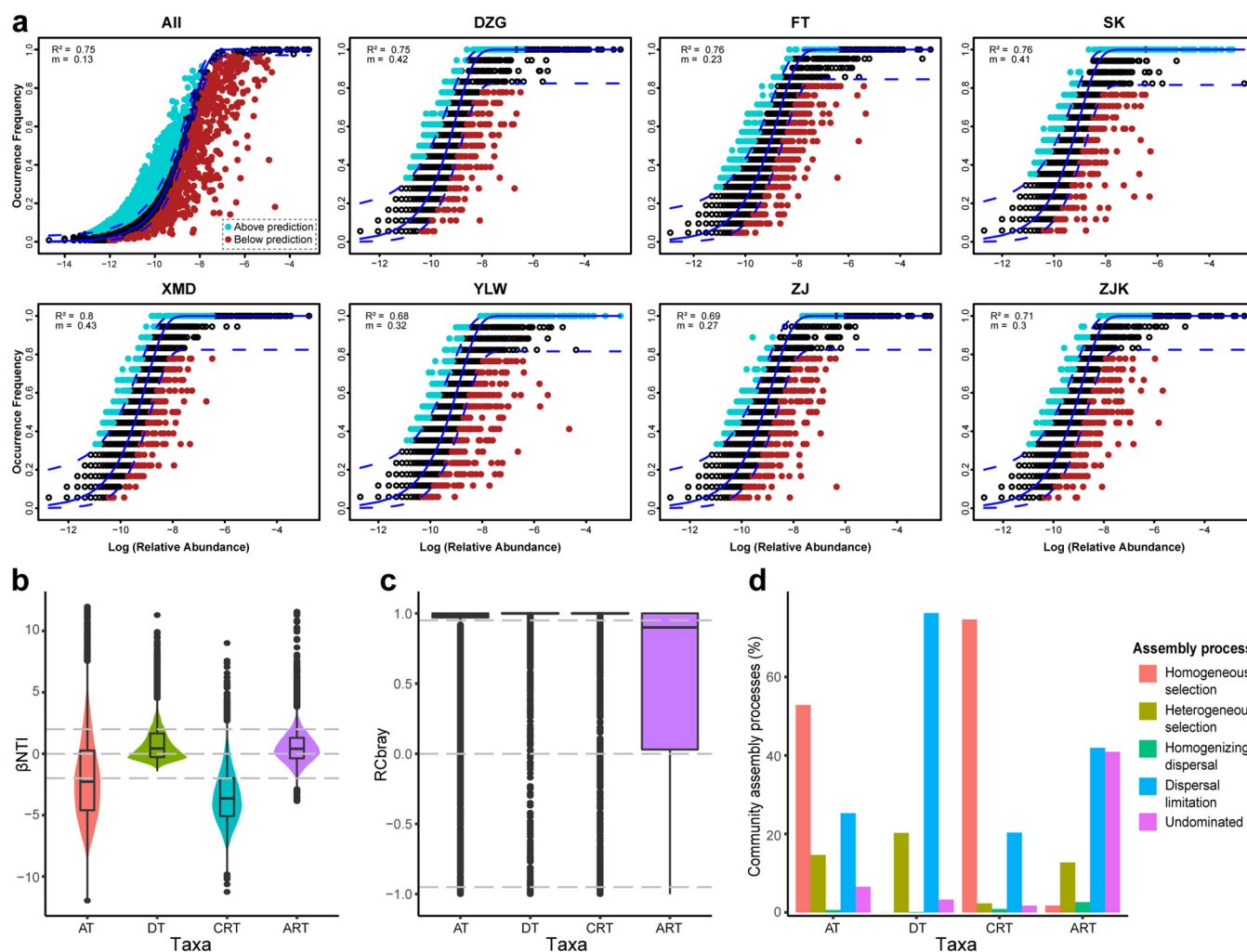


FIG 3 Archaeal community assembly patterns. (a) Fitting of the neutral community model (NCM) of community assembly in all and individual mangroves. Solid blue lines, the best fit to NCM. Dashed blue lines, 95% confidence interval for the prediction. OTUs that occur more or less frequently than predicted by the NCM are denoted by different colors. m , immigration rate; R^2 , fit to the model. (b) β -nearest-taxon index (β NTI) of all-taxon (AT), dominant taxon (DT), conditionally rare taxon (CRT), and always-rare taxon (ART) communities in all mangroves. Horizontal dashed lines (β NTI values at 2 and -2), thresholds of significance. (c) Bray-Curtis-based Raup-Crick (RC_{bray}) values of AT, DT, CRT, and ART communities in all mangroves. Horizontal dashed lines, RC_{bray} values at 0.95 and -0.95 . (d) The percent turnover of AT, DT, CRT, and ART community assembly governed primarily by various deterministic processes, including homogenous and heterogeneous selections, and stochastic processes, including dispersal limitations and homogenizing dispersal, as well as “Undominated” processes.

(Fig. 3a). The estimated immigration rate (m) was much higher in individual mangroves (0.23 to 0.43) than that in all mangroves (Fig. 3a), suggesting the occurrence of more dispersal events and ecological drift within each mangrove than among mangroves. To further explore the relative contribution of the stochastic and deterministic processes to the archaeal community assembly, β NTI and Bray-Curtis-based Raup-Crick (RC_{bray}) were calculated based on the OTU abundance and their phylogenetic distance. For all taxa, while the average β NTI value (-1.92) in all mangroves was slightly higher than -2 , the threshold of stochastic and deterministic processes, the majority of β NTI values (67.5%) in all mangroves were lower than -2 or higher than 2 (Fig. 3b). This indicated that the deterministic processes are more important for community assembly than the stochastic processes. Further, the majority (78.0%) of RC_{bray} values were greater than 0.95, indicating a more important role of dispersal limitation in the community assembly than that of homogenizing dispersal and “Undominated” processes (Fig. 3c). Consequently, based on the criteria described in Materials and Methods, all taxon community assembly patterns in mangroves were assigned to five portions: homogeneous selection, heterogeneous selection, homogenizing dispersal, dispersal

limitation, and “Undominated” processes. Of these, homogeneous selection (52.9%), followed by dispersal limitation (25.3%), was the most crucial process controlling the community assembly (Fig. 3d). Similarly, homogeneous selection played a crucial role in the conditionally rare taxon community assembly (Fig. 3b to d). In contrast, the dominant assembly process controlling the dominant taxon (76.3%) and always-rare taxon (41.9%) community assembly was dispersal limitation. The roles of “Undominated” processes (41.0%) in the always-rare taxon community assembly were almost equal to those of dispersal limitation (Fig. 3d). For each mangrove sampled in the current study, homogeneous selection was the dominant assembly process (38.2 to 64.7%), followed by dispersal limitation (19.7 to 33.5%) (Fig. S4a to c).

The correlations between β NTI values and changes in the environmental variables were further explored (Fig. S4d). β NTI values were significantly correlated with the changes of several variables, especially for the conditionally rare taxon community, for which the β NTI values were significantly correlated with all variables except for tidal height. Among the variables, changes in MAP and salinity were most strongly correlated with β NTI (Fig. S4d). However, all correlations were quite weak ($|R| < 0.22$) (Fig. S4d). Further, Bray-Curtis similarity values of archaeal communities (including all-taxon, always-rare taxon, conditionally rare taxon, and dominant taxon communities) in all samples and different depth layers were significantly and negatively correlated with the geographical distance, indicating a significant distance-decay relationship between them ($P < 0.001$, Fig. S5). In addition, Bray-Curtis similarity of the dominant taxon communities was significantly higher than that of the conditionally rare taxon and always-rare taxon communities, and that of the conditionally rare taxon communities was also significantly higher than that of the always-rare taxon communities, suggesting a stronger environmental preference or limitation of ecological dispersal of always-rare taxa than that of conditionally rare taxa and dominant taxa (Fig. S6).

Spatial and environmental selection shaping the archaeal community composition. Regarding the α -diversity indices, OTU richness was positively correlated with MAT, gravel proportion, pH, total nitrogen (TN), N/NO_3^- , and TS, but it was negatively correlated with latitude, longitude, depth, tidal height, and TP. Shannon index was positively correlated with gravel proportion, pH, N/NO_3^- , and TS but negatively correlated with N/NH_4^+ and TP (Table 1). Correlation analyses were further performed to explore the relationships between the environmental variables and the relative abundance of main phyla and classes (Table 1). The relative abundance of *Bathyarchaeota* was significantly positively correlated with sediment depth, MAT, and TS but negatively correlated with latitude, longitude, tidal height, pH, and N/NH_4^+ . The relative abundance of *Woeseearchaeota* was negatively correlated with depth, MAT, pH, and TS and positively correlated with latitude, longitude, and tidal height. Furthermore, the relative abundance of *Euryarchaeota* was significantly correlated with all variables except for depth, MAP, salinity, and total carbon (TC), among which it was negatively correlated with latitude, longitude, and tidal height. Depth, MAT, TC, TOC, and TS were significantly positively correlated with the relative abundance of Asgard archaea, while latitude, longitude, tidal height, and TP showed negative correlations (Table 1). The above observations indicated significantly lower archaeal richness in high-latitude mangroves than in low-latitude mangroves. Similarly, compared with low-latitude mangroves, the relative abundance of Asgard archaea, *Bathyarchaeota*, and *Euryarchaeota* was significantly reduced in high-latitude mangroves. However, the relative abundance of *Thaumarchaeota* and *Woeseearchaeota* was significantly higher at high latitudes than at low latitudes.

Bray-Curtis similarity-based principal-coordinate analysis (PCoA) revealed that, although the percentages on the x and y axes were very low, the archaeal communities of all taxa, dominant taxa, and conditionally rare taxa were generally clustered according to mangrove location (Fig. 4), which was further supported by permutational multivariate analysis of variance (PERMANOVA) of the archaeal community ($P = 0.001$, Fig. 4). While the percentages on the x and y axes of the PCoA plot of always-rare taxon communities were much lower than those of the other three plots, the PERMANOVA confirmed the significant difference of always-rare taxon communities in different

TABLE 1 Correlation coefficients (Spearman's rho) for the OTU richness, α -diversity, and relative abundance of main phyla and classes with environmental factors

Parameter/ phylum	Correlation coefficient (ρ) ^a															
	Latitude	Longitude	Depth	Tide	MAT	MAP	Gravel	Salinity	pH	TC	TOC	TN	N/NH ₄ ⁺	N/NO ₃ ⁻	TP	TS
OTU richness	-0.209**	-0.199*	-0.309***	-0.191*	0.219**	-0.108	0.239**	0.055	0.150*	0.128	0.121	0.211**	-0.042	0.218**	-0.180*	0.189*
Shannon-Wiener	-0.028	-0.008	-0.110	-0.030	0.043	-0.085	0.150*	0.055	0.148*	0.071	0.060	0.138	-0.199*	0.172*	-0.267**	0.156*
Chao1	-0.334***	-0.362***	-0.0410	-0.318***	0.316***	0.085	0.149*	-0.127	0.112	0.116	0.128	0.211**	0.065	-0.038	-0.060	0.203*
Evenness	0.026	0.0503	-0.040	0.017	-0.011	-0.072	0.112	0.044	0.131	0.053	0.042	0.110	-0.234**	0.150*	-0.280**	0.133
All A sgard phyla	-0.231**	-0.221**	0.423***	-0.253**	0.231**	0.064	0.018	-0.027	-0.043	0.152*	0.179*	0.133	-0.141	0.116	-0.302***	0.339***
Bathyrarchaeota	-0.253**	-0.249**	0.375***	-0.211**	0.237**	-0.086	0.032	-0.129	-0.181*	0.089	0.073	0.063	-0.316***	-0.007	-0.397***	0.204*
Euryarchaeota	-0.322***	-0.285***	0.018	-0.360***	0.374***	-0.016	0.326***	0.123	0.454***	0.184	0.217**	0.157*	0.626***	0.183*	0.322***	0.300***
Lokiarchaeota	-0.287**	-0.266**	0.407***	-0.321***	0.286***	0.113	0.025	-0.096	-0.090	0.188*	0.218**	0.150*	-0.125	0.092	-0.306***	0.362***
Micrarchaeota	-0.111	-0.099	-0.068	-0.172*	0.121	0.229**	0.014	-0.283***	0.029	0.083	0.082	0.161*	0.133	0.018	0.103	0.055
Odinarchaeota	-0.182*	-0.208**	0.103	-0.136	0.205*	-0.223**	0.101	0.187*	0.144	0.001	0.024	0.154*	-0.018	0.207**	-0.185*	0.171*
Thaumarchaeota	0.310***	0.289***	-0.376***	0.362***	-0.345***	-0.101	-0.243**	0.083	-0.139	-0.256**	-0.255**	-0.183*	-0.159*	-0.076	0.096	-0.440***
Woesearchaeota	0.356***	0.390***	-0.513***	0.296***	-0.335***	0.084	-0.087	-0.001	-0.204*	-0.044	-0.092	0.024	-0.028	-0.076	0.104	-0.249**
Methanomicrobia	-0.130	-0.062	-0.166*	-0.245**	0.164*	0.307***	0.130	-0.257**	0.165*	0.261**	0.261**	0.150*	0.489***	-0.053	0.331***	0.231**
Methanosarcinia	-0.110	-0.149*	-0.009	-0.088	0.129	-0.082	0.074	0.180*	0.275***	-0.031	-0.025	-0.049	0.593***	0.016	0.485***	0.008
Micrarchaeia	-0.111	-0.099	-0.068	-0.172*	0.121	0.229**	0.014	-0.283***	0.029	0.083	0.082	0.161*	0.133	0.018	0.103	0.055
Nitrososphaeria	0.310***	0.289**	-0.373***	0.362***	-0.345***	-0.101	-0.243**	0.083	-0.139	-0.256**	-0.255**	-0.183*	-0.159*	-0.076	0.096	-0.440***
Thermococci	-0.019	0.007	0.188*	-0.115	0.039	0.306***	0.090	-0.138	0.230**	0.091	0.104	0.074	0.226**	0.021	0.215**	0.226**
Thermoplasmata	-0.390***	-0.314***	-0.023	-0.403***	0.442***	-0.179*	0.414***	0.160*	0.302***	0.247**	0.293***	0.257**	0.150*	0.308***	-0.219**	0.342***

^aSignificance: *, $P \leq 0.05$; **, $P \leq 0.01$; ***, $P \leq 0.001$; ****, $P \leq 0.0001$.

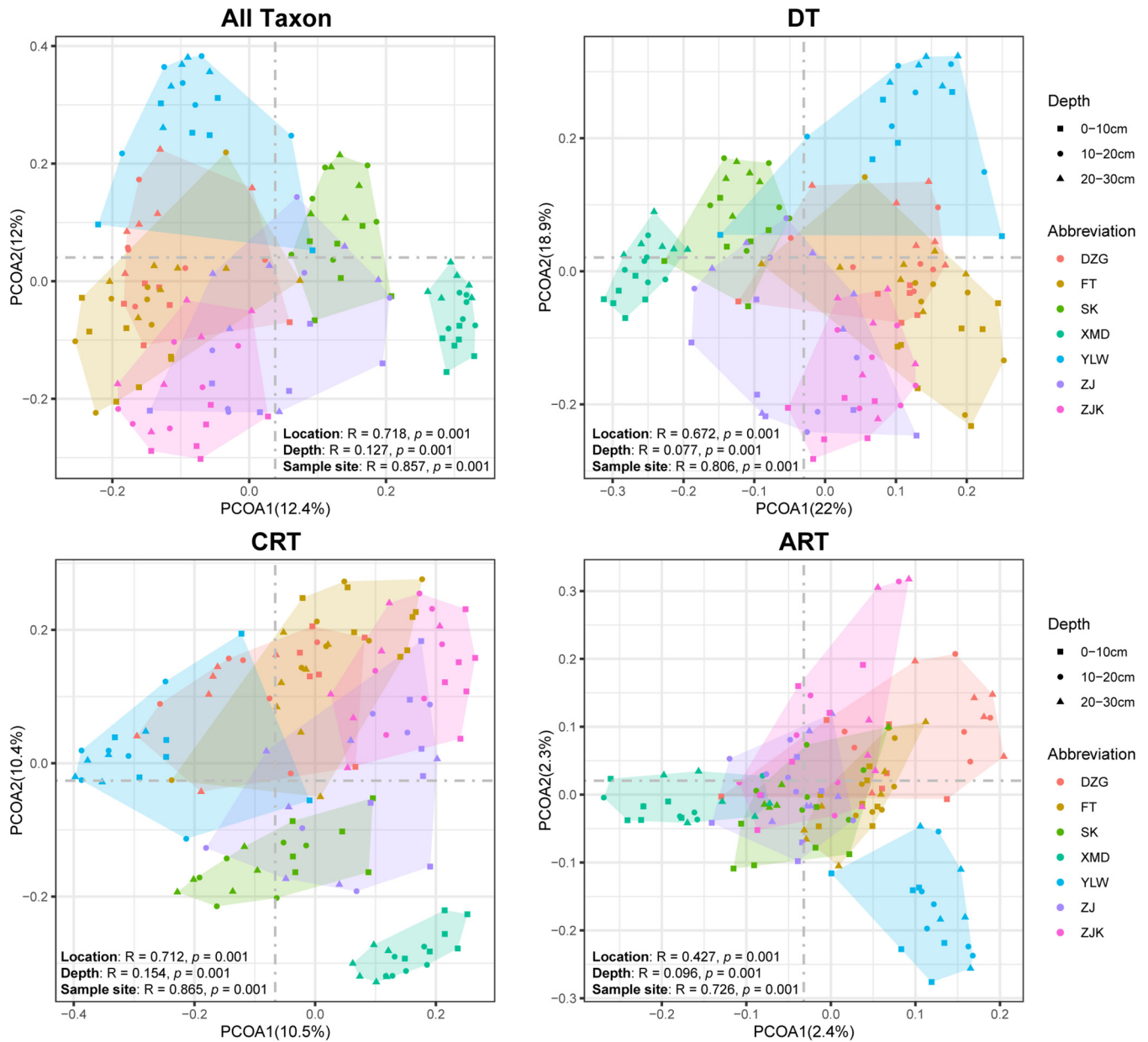


FIG 4 Principal-coordinate analysis (PCoA) derived from the Bray-Curtis dissimilarity matrices displaying the β -diversity of all taxon, dominant taxon (DT), conditionally rare taxon (CRT), and always-rare taxon (ART) communities. Similarity values among the samples of different mangroves (“Location”), depths (“Depth”), and sample sites (“Sample site”) were examined by using the analysis of similarities (ANOSIM) and are shown in the bottom right or left corner of each graph.

mangroves ($P = 0.001$, Fig. 4). This indicated significant differences in community composition between mangroves and similar biogeography of the dominant taxon, conditionally rare taxon, and always-rare taxon communities. PERMANOVA also confirmed significant differences in community composition between sample depths ($P = 0.001$) and sample sites ($P = 0.001$). In addition, either for all taxa or for dominant taxa, conditionally rare taxa, and always-rare taxa, sediment depth, location, latitude, longitude, and sample site significantly affected the archaeal communities ($P \leq 0.01$), and the effects of geographical location and sample site were much stronger than those of other spatial variables (Fig. 4; Fig. S7).

The VPA revealed 44.5% variations in the archaeal community explained by spatial and environmental variables. The explained variations of dominant taxon (49.8%) and conditionally rare taxon (33.7%) communities were much higher than that of the

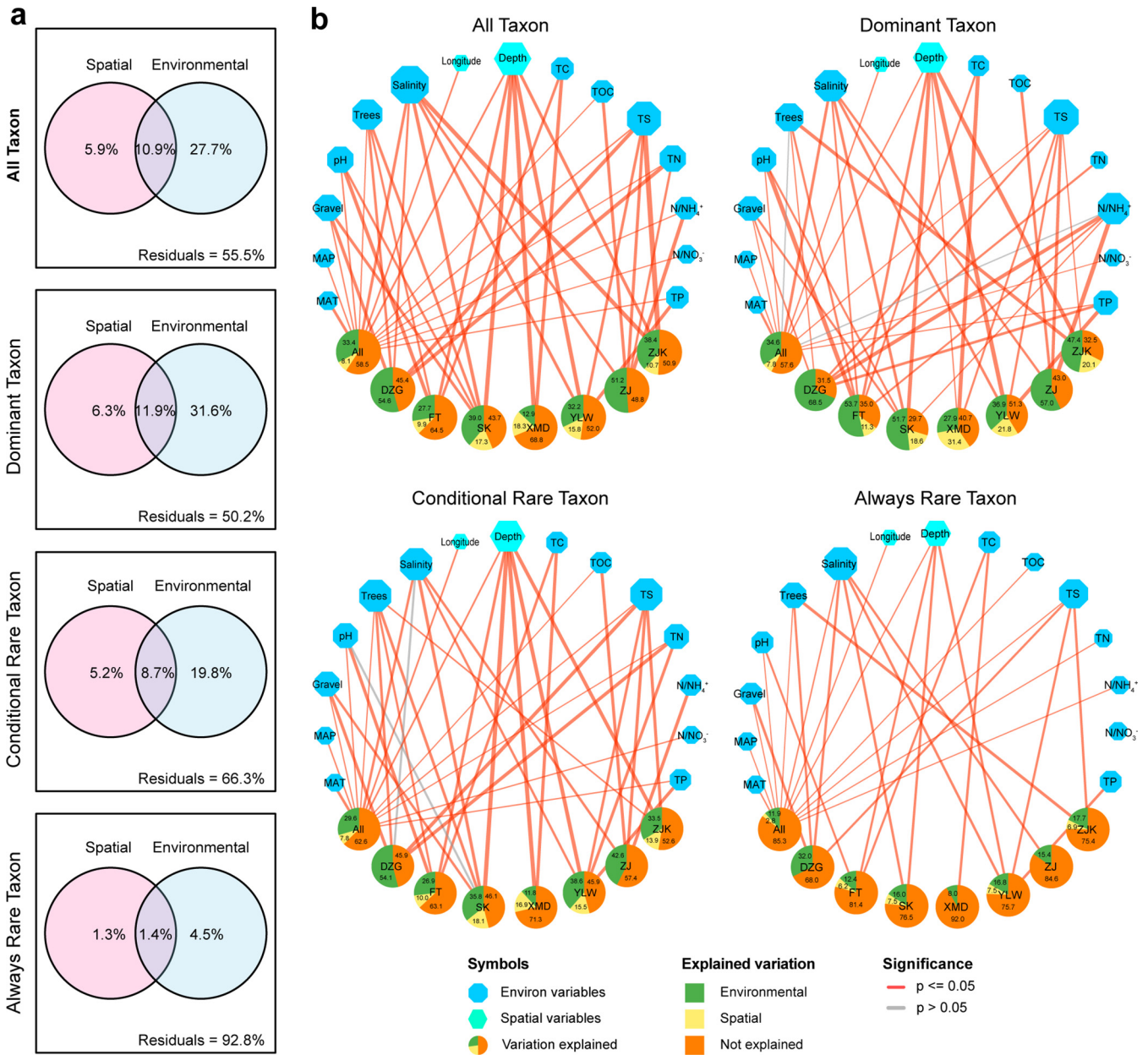


FIG 5 Effect of environmental selection on archaeal community composition. (a) Variation partition analysis based on Bray-Curtis dissimilarity matrices, partitioning the relative contributions of spatial and environmental factors to archaeal community structure. (b) Networks visualizing the results of distance-based redundancy analysis (db-RDA), exhibiting the effects of variables on the archaeal communities of all taxa, dominant taxa, conditionally rare taxa, and always-rare taxa. Upper blue hexagons and octagons, spatial and environmental factors, respectively. Their size represents the number of mangroves influenced by this factor. The bottom pie charts represent the variation of archaeal communities explained by variables in db-RDA models. Positive influences are displayed as red lines, and negative influences are in gray. The variation explained by each variable is displayed by the line width.

always-rare taxon community (7.2%) (Fig. 5a), which was further confirmed by db-RDA (Fig. 5b). All built db-RDA models were statistically validated using ANOVA. For all taxa, a model encompassing 14 variables (longitude, depth, gravel proportion, MAT, MAP, tree number, salinity, pH, TOC, TN, N/NH_4^+ , N/NO_3^- , TP, and TS) was built and explained 41.5% of the archaeal community variation (Fig. 5b). The explanations of models built for seven mangroves ranged from 31.2% (XMD) to 56.3% (SK). For dominant taxa, 12 variables were selected to build an overall community model, which explained slightly more variations (42.4%) than the all-taxon model. The models designed for dominant taxon communities in different mangroves explained 57.0% (ZJ) to 70.3% (SK) of community variation. Further, a model comprising 13 variables

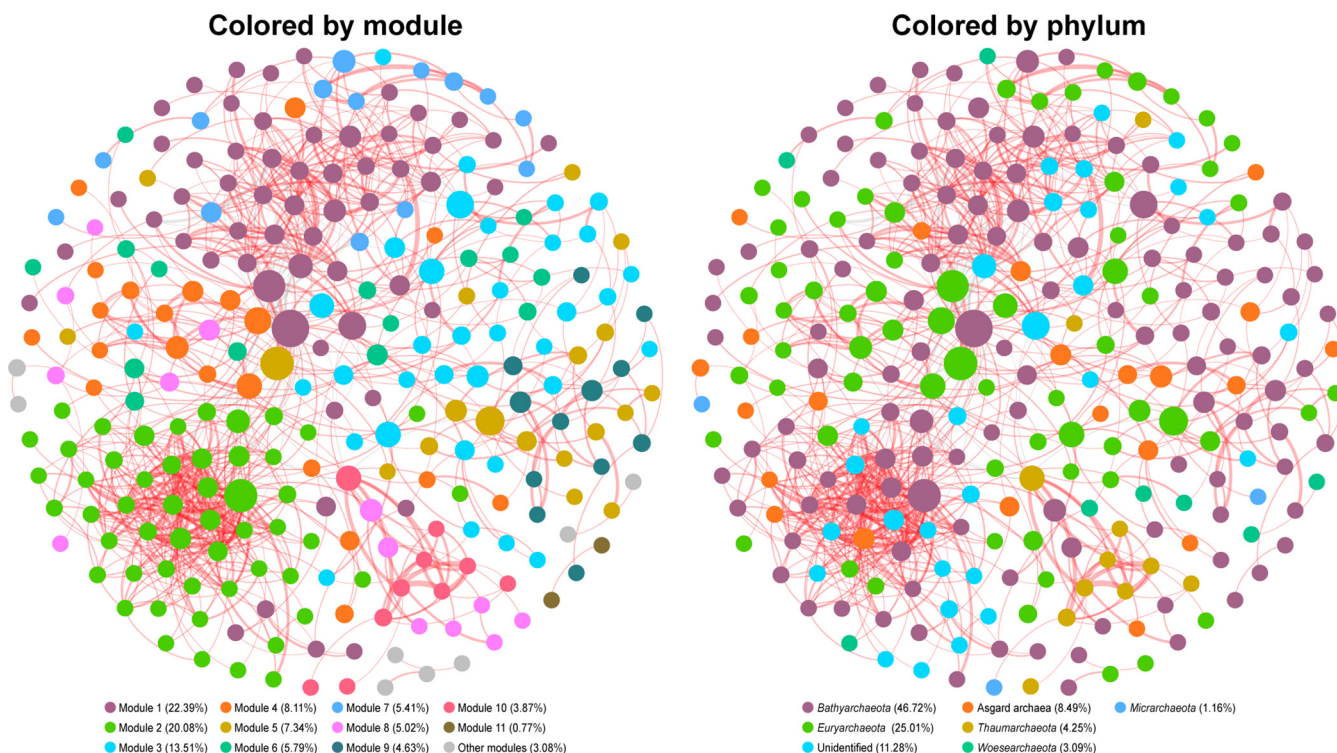


FIG 6 Cooccurrence networks of archaeal communities in all samples. Nodes of networks are colored according to the modularity class and phylum. Node size is proportional to the betweenness centrality of each node, and edge thickness is proportional to the MIC score of each correlation. Positive correlations are displayed as red lines, and negative correlations are in gray.

was constructed for the conditionally rare taxon community in all samples and explained 37.4% of all variation. The models for the conditionally rare taxon communities in different mangroves explained 28.7% (XMD) to 54.1% (DZG) of community variation. A 12-variable model was constructed for always-rare taxa in all samples, explaining 14.7% of variation; the models built for always-rare taxa in different mangroves explained 8.0% (XMD) to 32.0% (DZG) of community variation (Fig. 5b). Finally, in models built for the all-taxon, dominant taxon, conditionally rare taxon, and always-rare taxon communities, MAT and salinity were the most important factors shaping the archaeal community composition (Fig. 5b).

Cooccurrence patterns of archaeal community in mangrove sediments. Based on Spearman's correlation, a cooccurrence network consisting of 259 nodes (OTUs) and 830 edges was generated for the overall community (Fig. 6). This highly complex network had a diameter of 12, average degree (AD) of 3.21, modularity of 0.65, and average path length (APL) of 4.44. The network consisted of 15 modules, the top 10 of which accounted for 96.14% of the nodes (Fig. 6). The nodes in the network were assigned to six phyla, accounting for 88.72% of all nodes, with 11.28% remaining unidentified at phylum level (Fig. 6). Most edges (94.94%) in the network were positive, indicating that the cooccurring relationships accounted for almost the entire archaeal network (Fig. 6). According to the criteria specified in Materials and Methods, the top 10 OTUs with highest keystone scores listed in Data Set S1, sheet 3, were recognized as keystones. All the keystone taxa belonged to module 1 and module 2 (Data Set S1, sheet 3). Seven keystone taxa belonged to *Bathyarchaeota*, one belonged to Asgard archaea (*Lokiarchaeota*), and two were unidentified archaea.

DISCUSSION

***Bathyarchaeota*, *Euryarchaeota*, and *Woesearchaeota* are the predominant archaeal groups in mangrove sediments.** Similar to the observations of the current study, *Bathyarchaeota* are the predominant archaeal group also in other mangrove

sediments, accounting for up 40.2% of the overall archaeal community (12, 21, 22, 35). However, in some other reports, *Bathyarchaeota* are rare or almost entirely absent, with *Euryarchaeota* and *Thaumarchaeota* dominant (18, 36, 37). In a previous study on the archaeal diversity in DZG, a mangrove site also investigated in the current study, the relative abundance of *Crenarchaeota* was ca. 5 to 10% (36), which is much lower than that noted in the current study (29.6 to 61.7%, mean = 44.5%) and in another study based on the analysis of 16S rRNA gene clones (80.4%) (17). The primer pair 349F/806R used by Li et al. (36) allowed the retrieval of only 11 to 44% of archaeal sequences from each sample, while the Arch519F/Arch915R primers used in the current study retrieved 44.3 to 99.4% of archaeal sequences. The latter therefore provided a more accurate overview of the archaeal community in mangroves. On the other hand, the discrepancy in the reported distribution of *Bathyarchaeota* in different mangroves and samples might be associated with some environmental variables in mangrove wetlands (22). Here, in agreement with previous reports (7, 21, 22), the abundance of *Bathyarchaeota* in subsurface sediment was significantly higher than in surface sediment (see Fig. S3 in the supplemental material) and was positively correlated with sampling depth (Table 1). Further, many *Bathyarchaeota* OTUs were significantly enriched in subsurface sediments compared with surface sediments, while the number of depleted OTUs in subsurface sediments was especially low (Fig. 2a and b). Meanwhile, the Mantel test revealed significant effects of depth on the enriched *Bathyarchaeota* taxa, indicating that depth is a major factor shaping the *Bathyarchaeota* community, in addition to other variables, such as MAT, pH, and salinity (Fig. 2c; Table 1) (22, 38, 39).

Euryarchaeota are one of the most predominant archaeal groups, widely distributed in estuarine and mangrove sediments (13, 21, 22, 40). The wide distribution and high abundance of *Euryarchaeota* are a consequence of their pronounced degrading capabilities of diversified substrates and distinct niche adaptations (41–43). Another fascinating observation of the current study was the exceptionally high richness of *Woesearchaeota* (58.9% of all OTUs, 12.8% of sequences). High proportions of *Woesearchaeota* had been recovered from mangrove sediments worldwide, e.g., in China (22, 36, 44) and India (45). This might be attributable to their anaerobic heterotrophic lifestyle and diverse metabolic capabilities, such as the utilization of starch or sugar, acetate fermentation, and metabolism of hydrogen and nitrogen (33, 46), which made them flourish in mangrove sediments, a habitat with nutrient-rich and anaerobic conditions. Unlike *Bathyarchaeota*, the abundance of *Woesearchaeota* in surface sediments was significantly higher than in subsurface sediments and was negatively correlated with sediment depth, indicating that depth significantly impacts the *Woesearchaeota* community, which might be associated with the niche preference of *Woesearchaeota* members (46).

Homogeneous selection controls archaeal community assembly in mangrove sediments. The β NTI analysis supported a relatively more crucial role of deterministic processes than that of stochastic processes, either in all (Fig. 3b to d) or in individual (Fig. S4c) mangroves (23, 25, 47). Homogeneous selection is a selection under homogeneous abiotic and biotic environmental conditions that leads to increasingly similar structures of various communities (25). Hence, the dominant homogeneous selection observed in the current study might be an outcome of homogenized mangrove habitat (48). However, according to one study of prokaryotic communities in mangrove sediments, heterogeneous selection (β NTI > 2) and stochastic processes ($|\beta$ NTI| < 2) are dominant in all and individual mangroves, respectively (13). This inconsistency might stem from the notion that only OTUs with an overall abundance above 0.01%, representing the dominant taxa and most conditionally rare taxa, were considered in the previous study, with sediment samples around *Spartina alterniflora*, an invading marsh grass, included in the analysis (16). The β NTI analysis also revealed an important role of stochastic processes in community assembly, in all and in individual mangroves (Fig. 3d; Fig. S4c). Consistent with the work of Zhang et al. (13), the high fitness of NCM to the archaeal communities in all and individual mangroves (Fig. 3a) indicates the importance of stochastic processes for archaeal community structure (13, 26). Further,

regarding the estimated archaeal community immigration rate, the m values in each mangrove were higher than that for all mangroves (Fig. 3a), indicating that the dispersal ability of most archaeal taxa within an individual mangrove was higher than that between mangroves. These observations might be attributed to the dispersal limitation and ecological drift that are strongly positively correlated with geographical distance (Fig. S5). Because of the dispersal limitation and ecological drift, longer distance will generate stronger environmental selection, dispersal limitation, and ecological drift and thus results in a distance-decay community similarity (49, 50).

In the current study, dominant taxon communities were mainly driven by dispersal limitation. This result supported prior reports that dominant taxa were mainly limited by dispersion in lakes and reservoirs in China (51), the northwestern Pacific Ocean (52), and agricultural fields in China (48, 53). There are two possible explanations. First, more-abundant species have a greater probability of dispersal than less-abundant species (25, 53). Second, dominant taxa are supposed to have wide niche breadth, and these taxa with wide breadth may be limited by the possibilities to reach multiple locations (dispersal limitation). On the other hand, taxa with narrow niche breadths (rare taxa) may face strong negative environmental selection (52, 54). However, other researchers have also noted stronger limitation of rare taxa than the abundant taxa by dispersal in oil-contaminated soils (55) and subtropical bays (56). These discrepancies may be associated with the difference in the habitat and geographical location (48). The high fraction of “Undominated” processes (41.0%) that contributed to the always-rare taxon community assembly indicates that the always-rare taxon community might be shaped by highly complex assembly mechanisms (48, 56). In summary, we suggest that homogeneous selection strongly shapes the overall and conditionally rare taxon archaeal community assembly and that the stochastic processes play crucial roles in the dominant taxon and always-rare taxon community assembly in mangrove sediments.

Environmental selection plays a moderate role in shaping archaeal community in mangrove sediments. In the current study, PCoA revealed distinct community compositions between mangroves; high community similarity within the same mangrove; and similar biogeography of the dominant taxon, conditionally rare taxon, and always-rare taxon archaea in mangrove sediments (Fig. 4). In agreement with these observations, Zhang et al. (13) reported a similar geographical distribution of the prokaryotic community in mangrove sediments, indicating a crucial role of geographical location in shaping archaeal communities in mangrove sediments. The pronounced effects of geographical location are possibly associated with the combined effects of climate, niche conservatism, and rates of dispersal, evolutionary radiation, and extinction in different environments (34, 57). Although the always-rare taxon community did not cluster as well as the all-taxon, dominant taxon, and conditionally rare taxon communities, PERMANOVA supported significant differences between always-rare taxon communities among mangroves (Fig. 4). This was supported by the distance-decay relationship of community similarity and geographical distance (Fig. S5). Similar observations have been made for bacterial communities in coastal Antarctic lakes (58), subtropical bays (56), and microeukaryotic communities in rivers (26).

Consistent with previous studies on fungal, microeukaryotic, or prokaryotic communities in different ecosystems (26, 56, 59, 60), the VPA and db-RDA model built in the current study explained a moderate proportion of variations in all taxon and dominant taxon communities and a relatively low proportion of variations in the conditionally rare taxon and always-rare taxon communities. This indicates a relatively important role of environmental and spatial factors in shaping the all-taxon and dominant taxon communities but a minor role in shaping the conditionally rare taxon and always-rare taxon communities (Fig. 5). Specifically for always-rare taxa, the variables explained only 7.2% (VPA) or 14.7% (db-RDA) of community variation (Fig. 5). As suggested by Chen et al. (26), this observation has several potential explanations. First, some other, more important factors may exist that are not accounted for in the current study. Second, cooccurrence relationships among microbes that significantly affect the community composition cannot be quantified by VPA or db-RDA (61, 62). Third, in some

studies, VPA failed to correctly predict the explained community variation and thus should be used together with other approaches, such as NCM (25). Furthermore, for all taxa, always-rare taxa, conditionally rare taxa, and dominant taxa, db-RDA explained a greater proportion of community variation in each mangrove than in all mangroves (Fig. 5), indicating a stronger environmental selection acting on the archaeal community on a small geographical scale rather than a large scale. In conclusion, the above observations reveal similar biogeography of the all-taxon, dominant taxon, conditionally rare taxon, and always-rare taxon communities, a major effect of mangrove location, and a moderate role of environmental selection in driving the archaeal community structure in mangrove sediments.

Cooccurrence network patterns and keystone taxa in archaeal community in mangrove sediments. In natural ecosystems, microorganisms preferentially form complex interaction networks rather than thrive in isolation (63). The microbial community composition and dynamics are significantly affected by microbial interactions, and a cooccurrence network constructed using correlation coefficient metrics can provide evidence of interaction between species, such as antagonism or cooperation (61, 62, 64). The mostly positive correlations in the cooccurrence network determined in the current study indicate the possibility that synergy in archaeal communities in mangrove sediments is more frequent than antagonism (64). This phenomenon is quite often observed in natural ecosystems and perhaps is not surprising, because many microbes highly depend on cross-feeding, coaggregation, cocolonization, or niche overlap and construction (65–67). Using anaerobic digesters, Chouari et al. (68) observed a clear cooccurrence of *Crenarchaeota*, *Thermoplasmata*, and methanogens. Consistently, in modules 1 to 5 defined in the current study, close correlations between *Bathyarchaeota* and *Thermoplasmata* or among *Bathyarchaeota*, *Thermoplasmata*, and *Methanomicrobia* were observed (Fig. S8). They indicate that closely cooperative and synergistic interactions might be among these archaea (68). In the current study, seven of the 10 identified keystones were *Bathyarchaeota*. It has been suggested that members of *Bathyarchaeota* can utilize protein, cellulose, short-chain hydrocarbons, and some other recalcitrant organic matters (69). Some *Bathyarchaeota* lineages even have the ability to fix CO₂ and engage in methane metabolisms (15, 69, 70). Meanwhile, more than 46% of nodes in the overall network represented *Bathyarchaeota*, suggesting that *Bathyarchaeota* might be crucial components maintaining the ecological function and completeness of the archaeal community and playing important roles in the nutrient and biogeochemical cycling in mangrove sediments.

Although only archaeal communities in mangrove sediment in China were analyzed in the current study, it would be useful to compare the archaeal communities in mangrove sediment and mudflats in different countries. Meanwhile, an annual or seasonal monitoring or average might be more appropriate and precise to demonstrate the structure of the archaeal community in mangroves. However, the above works were not performed here, for several reasons. First, Pan et al. (22) had compared the archaeal communities in mangroves and mudflat sediments in the Futian mangrove in China and observed that the archaeal communities were more similar in the same environments than those in different environments. Second, due to the different PCR primers used in previous studies (7, 71), comparisons between mangroves in China and reported countries were not performed, which may generate bias results due to the different specificities of these primers. Finally, the limited budget of the current study prevented us from the annual and overseas samplings. In the future, temporal variation across seasons and years and spatial variation across continent(s) should be explored to show the overview of archaeal community in mangroves.

Conclusions. In conclusion, we found higher archaeal diversity in surface mangrove sediments than in subsurface sediments. *Woesearchaeota* and *Bathyarchaeota* exhibited the highest OTU richness and relative abundance, respectively. In subsurface sediment layers, *Woesearchaeota* were mainly depleted, while *Bathyarchaeota* were largely enriched. Meanwhile, archaeal communities in low-latitude mangroves were significantly more diverse than those in high-latitude mangroves. β NTI analysis and NCM

modeling suggested that homogeneous selection strongly shapes the overall and conditionally rare taxon community assembly, whereas stochastic processes play crucial roles in the dominant taxon and always-rare taxon community assembly. PCoA and PERMANOVA revealed similar distribution and biogeography of the all-taxon, dominant taxon, conditionally rare taxon, and always-rare taxon communities. Further, both VPA and db-RDA revealed moderate proportions of community variation explained by spatial and environmental variables. The effects of environmental selection on the always-rare taxon community were weaker than those on dominant taxa and conditionally rare taxa. Mangrove location, MAT, and salinity are the major variables affecting the archaeal community composition. Finally, network analysis revealed comprehensive cooccurrence relationships within an archaeal community, with possible cooperative and synergistic interactions. *Bathyarchaeota* were crucial components of the archaeal community. Overall, these findings provide novel important information on the biogeography, assembly patterns, driving factors, and cooccurrence relationships of archaeal community in mangrove sediments.

MATERIALS AND METHODS

Sediment sample collection and variable analysis. Sediment samples were collected at seven representative mangrove nature reserves in Southeast China in October to November 2019 (see Data Set S1, sheet 1, in the supplemental material). Briefly, six (all except FT) or seven (FT) sampling sites located at the same distance from each other were selected in each mangrove. To compare the vertical profiles of archaeal communities, sediment samples were collected using a stainless-steel sampler and separated into three depth layers (oxic fraction, 0 to 10 cm; anoxic fraction, 10 to 20 cm; and 20- to 30-cm layers) at each sampling sites, according to the criteria of Luis et al. (7). To reduce sampling bias, three replicates were collected at the vertices of an equilateral triangle and mixed together for each site. Overall, 127 sediment samples were collected (Data Set S1, sheet 1).

Data on the spatial and environmental variables are summarized in Data Set S1, sheet 1. The spatial variables included sampling depth, longitude, latitude, and the number of tree species within 5 m of the sampling site. The environmental variables, i.e., tidal height (<https://www.cnss.com.cn/tide/>), MAT, MAP (obtained from the China Meteorological Administration [<http://www.cma.gov.cn>]), salinity, pH, gravel proportion, TC, TOC, TN, N/NH₄⁺, N/NO₃⁻, TP, and TS, were determined as described by Zhang et al. (60).

DNA extraction, sequencing, and data processing. Sediment genomic DNA was extracted from an 0.3-g sample using DNeasy PowerSoil kit (Qiagen, Germany) according to the manufacturer's instructions. The quantity and quality of extracted DNA were examined using a NanoDrop ND-2000 spectrophotometer (NanoDrop Technologies, USA). The DNA samples were stored at -40°C before amplification by PCR. The hypervariable region 4 (V4) of the archaeal 16S rRNA gene was amplified using the primer pair Arch519F/Arch915R (72, 73). PCR-free libraries were constructed from the 16S rRNA gene amplicons and sequenced using the HiSeq Xten platform with a 450-bp single-end strategy (Illumina, San Diego, CA, USA) at Novogene (Beijing, China).

Raw reads were quality filtered (-q = 20) using Sickle (74). The subsequent replication, singleton and chimera removal, and OTU clustering (at 97% similarity) were performed using USEARCH (75, 76). Taxonomic information for each OTU was assigned by aligning the representative sequences with those deposited in SILVA Nr99 (v138) (77) using BLASTn (78). Bacterial OTUs were removed, and archaeal OTUs were retained. To minimize bias associated with sequencing coverage, the resultant OTU table was rarefied to 19,206 sequences per sample for downstream analyses. The relative abundance of individual taxa was calculated by comparing the read number of each taxon with the total read number in that sample. In the current study, all archaeal OTUs (all taxa) were classified into three categories: dominant taxa, OTUs with the relative abundance of $\geq 0.01\%$ in all samples or $\geq 1\%$ in some samples; always-rare taxa, OTUs with the abundance of $< 0.01\%$ in all samples; and conditionally rare taxa, with the abundance of $< 1\%$ in all samples and $< 0.01\%$ in some samples (26, 28).

Statistical analysis. (i) Different taxa in subsurface sediments. Enriched and depleted OTUs in subsurface-layer samples (10 to 30 cm) compared with surface-layer samples (0 to 10 cm) were analyzed using metagenomeSeq package (79). Using a log transformation [$\log_2(y_{ij} + 1)$] followed by correction for zero-inflated log-normal model, metagenomeSeq was specifically designed for the differential abundance analysis of amplicon sequencing and had a substantially best performance for microbial marker-gene surveys (79, 80). According to the work of Paulson et al. (81), a zero-inflated log-normal model implemented in the fitFeatureModel function in the metagenomeSeq package was used for the differential abundance testing for OTUs in surface and subsurface sediments. The effects of spatial and environmental variables on the enriched and depleted OTUs in subsurface sediments were explored using the Mantel test in vegan package (82), to determine Spearman's correlation coefficient between the Bray-Curtis distance of enriched or depleted OTUs and Euclidean distance of spatial and environmental variables based on 9,999 permutations.

(ii) α - and β -diversity analysis. α -Diversity indices, including OTU richness, Shannon-Wiener, Chao1, and evenness indices, were calculated using the vegan package (82). ANOVA followed by Tukey's honestly significant difference method was used to explore the variations of α -diversity and relative abundances of major phyla across different depths (83). Pearson's correlation coefficients and *P* values

were calculated to explore the associations between α -diversity, main archaeal phyla and classes, and environmental features. The distance matrix of the archaeal community (Hellinger transformation of the OTU abundance data) was constructed by calculating dissimilarity using the Bray-Curtis method (82). In the current study, PCoA was employed using the Bray-Curtis similarity matrices to visualize shifts in different archaeal community compositions. Significant differences ($P < 0.05$) among groups were evaluated using the analysis of similarities (ANOSIM).

(iii) Archaeal community assembly patterns. NCM was used to determine the potential roles of stochastic processes in archaeal community assembly by predicting the relationship between OTU detection frequency and the OTU's relative abundance in the whole community (26, 84, 85). The model used here is derived from the neutral theory (25, 26). The model predicts that taxa that are abundant in the community will be widespread, since they are more likely to disperse by chance among different sampling sites, while rare taxa are more likely to be lost due to the ecological drift (26). In this model, parameter m represents the immigration rate, and R^2 represents the overall fit to the neutral model. The `snm.fit_function.r` script written by Burns et al. (86) was used to evaluate the NCM fit. Further, Pearson's correlation coefficients between Bray-Curtis similarity of the archaeal community and geographic distance of the samples were calculated to determine the spatial predictor of archaeal community composition. The geographical distance (in km) between samples, i.e., a straight-line distance between the sampling points, was calculated using the package `geosphere` (87) based on the longitude and latitude coordinates of each sampling site.

To quantify the relative importance of stochastic and deterministic processes that drive the archaeal community assembly, the null model analysis was performed using Rscript `bNTI_Local_Machine.r` written by Stegen et al. (23), based on the phylogenetic distance and OTU abundance. This method can be used to detect community assembly mechanisms by estimating the standard deviation of the observed ecological patterns compared to the randomly shuffled ecological patterns produced by null models (23, 47). If the observed ecological patterns are not statistically different from null expectations, the community dynamics are largely considered stochastic; otherwise, they are regarded as deterministic (53). Briefly, β NTI is the number of standard deviations of the beta mean nearest taxon distance (β MNTD) from the mean of the null distribution (23). The RC_{bray} value was used to further partition pairwise comparisons that were assigned to stochastic processes (23, 25, 53). The β NTI values between -2 and 2 indicate dominance of the stochastic processes, whereas β NTI values smaller than -2 or larger than 2 indicate that deterministic processes (i.e., homogeneous selection and heterogeneous selection) play a more important role in community assembly than stochastic processes (13, 23, 25, 53). For $|\beta$ NTI| < 2 , $RC_{\text{bray}} < -0.95$ and $RC_{\text{bray}} > 0.95$ indicate relative dominant influence of homogenizing dispersal and dispersal limitation, respectively, and $|RC_{\text{bray}}| < 0.95$ indicates a crucial role of "Undominated" assembly, including weak selection, weak dispersal, diversification, and/or drift (25, 53, 88). The major factors that influence the assembly of dominant taxa, conditionally rare taxa, and always-rare taxa were explored separately. Pearson's correlation coefficients and P values were calculated to explore the associations between β NTI values and changes in environmental variables in different samples.

(iv) Archaeal community-driving factors. VPA based on db-RDA was performed to determine the relative proportions of community variation that could be explained by spatial (latitude, longitude, and sediment depth) and environmental (MAT, MAP, salinity, pH, gravel proportion, TC, TOC, TN, N/NH_4^+ , N/NO_3^- , TP, and TS) variables combined. To assess the relative impact of each variable on archaeal community structure, db-RDA with Bray-Curtis dissimilarity analysis was performed, exploring the community variations explained by spatial and environmental variables (89). Using `vif.cca` and `ordiR2step` function in the `vegan` package (82), the method described by Zhang et al. (60) was used to select parameters for the db-RDA model. Briefly, the final db-RDA model was comprised of variables forward-selected by `ordiR2step` with variance inflation factor (VIF) values below 10. The significance of the final model, axes, and terms was tested using the ANOVA command.

(v) Network patterns and keystone taxa of archaeal communities. Network analysis reveals the interactions within an archaeal community and keystone taxa within cooccurrence networks that are crucial for the composition and assembly of the community (64). The cooccurrence patterns in archaeal communities were determined by performing network analysis using the maximal information coefficient (MIC) scores (90). The MIC is a useful score that reflects the strength of linear and nonlinear associations among variables (90). To reduce the influence of false positives caused by OTU sparsity, OTUs that were present in at least half of the samples (i.e., 50% OTU sparsity) were included (91), resulting in 534 OTUs. The pairwise MIC associations were analyzed in `MICtools` with default parameters (92), and the P value was adjusted using false-discovery rate correction. Of the correlations, only those with adjusted P values below 0.001 were considered statically robust. Since MIC roughly equals the coefficient of determination R^2 between two variables (85, 90, 92), a MIC cutoff of 0.5, which represented a relatively strong coefficient ($|R| > 0.7$), was selected to construct the network (93). Meanwhile, the MIC cutoff also generated a moderate network size, 259 nodes and 830 edges. Cooccurrence networks were built using the `igraph` package (94); calculation of network topological properties and network visualization were performed using the interactive platform `Gephi v0.92` (95). In the network, a degree represents the number of edges connected to a node. Closeness centrality (CC) is based on the average shortest paths and thus reflects the central importance of a node in disseminating information (63). Betweenness centrality (BC) reveals the role of a node as a bridge between network components. Keystone species are defined as highly connected species that have a disproportionately large effect on the complexity of a community relative to their abundance (64, 96). Keystone taxa were OTUs with the highest degree and CC scores and the lowest BC score (64). Putative keystone OTUs in the networks were identified by calculating a keystone score by the average of degree, $1-BC$ score, and CC score after Mix-Max scaling (64, 97, 98).

Data availability. All raw sequences from the current study have been deposited in NODE (<http://www.biosino.org/node>) under the accession number OEP001412.

SUPPLEMENTAL MATERIAL

Supplemental material is available online only.

FIG S1, JPG file, 2 MB.

FIG S2, JPG file, 0.8 MB.

FIG S3, JPG file, 1.8 MB.

FIG S4, JPG file, 1.5 MB.

FIG S5, JPG file, 2.5 MB.

FIG S6, JPG file, 0.7 MB.

FIG S7, JPG file, 1.8 MB.

FIG S8, JPG file, 1.6 MB.

DATA SET S1, XLSX file, 9.1 MB.

ACKNOWLEDGMENTS

We thank Cui-Xing Ye (Hainan Academy of Ocean and Fisheries Sciences), Wen-Lu Lan (Guangxi Marine Environment Monitoring Centre station), Chun-Fang Zheng (Wenzhou University), and Jian-Biao Chou (Zhejiang Mariculture Research Institute) for help with sample collection. We acknowledge Joanna Mackie for providing professional editing services.

This work was financially supported by the National Natural Science Foundation of China (grant no. 31970105, 91851105); the Shenzhen Science and Technology Program (grant no. JCYJ20200109105010363); the Innovation Team Project of Universities in Guangdong Province (grant no. 2020KCXTD023), the National Science and Technology Fundamental Resources Investigation Program of China (grant no. 2019FY100700), and the China Postdoctoral Science Foundation (grant no. 2020M672779).

Z.-F.Z. and M.L. conceived the study. Z.-F.Z. and Y.-P.P. collected the sediment samples. Z.-F.Z. performed the laboratory experiments with the help of Y.-P.P. Z.-F.Z. analyzed the data and wrote the paper. M.L. and J.P. revised the manuscript. All authors read and approved the final manuscript.

REFERENCES

- Giri C, Ochieng E, Tieszen LL, Zhu Z, Singh A, Loveland T, Masek J, Duke N. 2011. Status and distribution of mangrove forests of the world using earth observation satellite data. *Glob Ecol Biogeogr* 20:154–159. <https://doi.org/10.1111/j.1466-8238.2010.00584.x>.
- Alongi DM. 2014. Carbon cycling and storage in mangrove forests. *Annu Rev Mar Sci* 6:195–219. <https://doi.org/10.1146/annurev-marine-010213-135020>.
- Donato DC, Kauffman JB, Murdiyarto D, Kurnianto S, Stidham M, Kanninen M. 2011. Mangroves among the most carbon-rich forests in the tropics. *Nat Geosci* 4:293–297. <https://doi.org/10.1038/ngeo1123>.
- Friesen SD, Dunn C, Freeman C. 2018. Decomposition as a regulator of carbon accretion in mangroves: a review. *Ecol Eng* 114:173–178. <https://doi.org/10.1016/j.ecoleng.2017.06.069>.
- Deborde J, Marchand C, Molnar N, Patrona L, Meziane T. 2015. Concentrations and fractionation of carbon, iron, sulfur, nitrogen and phosphorus in mangrove sediments along an intertidal gradient (semi-arid climate, New Caledonia). *J Mar Sci Eng* 3:52–72. <https://doi.org/10.3390/jmse3010052>.
- Lin X, Hetharua B, Lin L, Xu H, Zheng T, He Z, Tian Y. 2019. Mangrove sediment microbiome: adaptive microbial assemblages and their routed biogeochemical processes in Yunxiao Mangrove National Nature Reserve, China. *Microb Ecol* 78:57–69. <https://doi.org/10.1007/s00248-018-1261-6>.
- Luis P, Saint-Genis G, Vallon L, Bourgeois C, Bruto M, Marchand C, Record E, Hugoni M. 2019. Contrasted ecological niches shape fungal and prokaryotic community structure in mangroves sediments. *Environ Microbiol* 21:1407–1424. <https://doi.org/10.1111/1462-2920.14571>.
- Zhang C-J, Chen Y-L, Sun Y-H, Pan J, Cai M-W, Li M. 2021. Diversity, metabolism and cultivation of archaea in mangrove ecosystems. *Mar Life Sci Technol* 3:252–262. <https://doi.org/10.1007/s42995-020-00081-9>.
- Marcos MS, Barboza AD, Keijzer RM, Laanbroek HJ. 2018. Tide as steering factor in structuring archaeal and bacterial ammonia-oxidizing communities in mangrove forest soils dominated by *Avicennia germinans* and *Rhizophora mangle*. *Microb Ecol* 75:997–1008. <https://doi.org/10.1007/s00248-017-1091-y>.
- Liu Y, Zhou Z, Pan J, Baker BJ, Gu JD, Li M. 2018. Comparative genomic inference suggests mixotrophic lifestyle for Thorarchaeota. *ISME J* 12:1021–1031. <https://doi.org/10.1038/s41396-018-0060-x>.
- Cai M, Liu Y, Yin X, Zhou Z, Friedrich MW, Richter-Heitmann T, Nimzyk R, Kulkarni A, Wang X, Li W, Pan J, Yang Y, Gu JD, Li M. 2020. Diverse Asgard archaea including the novel phylum Gerdarchaeota participate in organic matter degradation. *Sci China Life Sci* 63:886–897. <https://doi.org/10.1007/s11427-020-1679-1>.
- Meng J, Xu J, Qin D, He Y, Xiao X, Wang F. 2014. Genetic and functional properties of uncultivated MCG archaea assessed by metagenome and gene expression analyses. *ISME J* 8:650–659. <https://doi.org/10.1038/ismej.2013.174>.
- Zhang CJ, Pan J, Duan CH, Wang YM, Liu Y, Sun J, Zhou HC, Song X, Li M. 2019. Prokaryotic diversity in mangrove sediments across southeastern China fundamentally differs from that in other biomes. *mSystems* 4:e00442-19. <https://doi.org/10.1128/mSystems.00442-19>.
- Lyimo TJ, Pol A, Jetten MS, den Camp HJ. 2009. Diversity of methanogenic archaea in a mangrove sediment and isolation of a new *Methanococoides* strain. *FEMS Microbiol Lett* 291:247–253. <https://doi.org/10.1111/j.1574-6968.2008.01464.x>.
- Pan J, Zhou Z, Beja O, Cai M, Yang Y, Liu Y, Gu JD, Li M. 2020. Genomic and transcriptomic evidence of light-sensing, porphyrin biosynthesis, Calvin-Benson-Bassham cycle, and urea production in Bathyarchaeota. *Microbiome* 8:43. <https://doi.org/10.1186/s40168-020-00820-1>.

16. Zhou Z, Liu Y, Lloyd KG, Pan J, Yang Y, Gu JD, Li M. 2019. Genomic and transcriptomic insights into the ecology and metabolism of benthic archaeal cosmopolitan, *Thermopfundales* (MBG-D archaea). *ISME J* 13:885–901. <https://doi.org/10.1038/s41396-018-0321-8>.
17. Yan B, Hong K, Yu ZN. 2006. Archaeal communities in mangrove soil characterized by 16S rRNA gene clones. *J Microbiol* 44:566–571.
18. Bhattacharyya A, Majumder NS, Basak P, Mukherji S, Roy D, Nag S, Haldar A, Chattopadhyay D, Mitra S, Bhattacharyya M, Ghosh A. 2015. Diversity and distribution of Archaea in the mangrove sediment of Sundarbans. *Archaea* 2015:968582. <https://doi.org/10.1155/2015/968582>.
19. Wang YF, Feng YY, Ma X, Gu JD. 2013. Seasonal dynamics of ammonia/ammonium-oxidizing prokaryotes in oxic and anoxic wetland sediments of subtropical coastal mangrove. *Appl Microbiol Biotechnol* 97:7919–7934. <https://doi.org/10.1007/s00253-012-4510-5>.
20. Wang L, Huang X, Zheng TL. 2016. Responses of bacterial and archaeal communities to nitrate stimulation after oil pollution in mangrove sediment revealed by Illumina sequencing. *Mar Pollut Bull* 109:281–289. <https://doi.org/10.1016/j.marpolbul.2016.05.068>.
21. Zhou Z, Meng H, Liu Y, Gu JD, Li M. 2017. Stratified bacterial and archaeal community in mangrove and intertidal wetland mudflats revealed by high throughput 16S rRNA. *Front Microbiol* 8:2148. <https://doi.org/10.3389/fmicb.2017.02148>.
22. Pan J, Chen Y, Wang Y, Zhou Z, Li M. 2019. Vertical distribution of bathyarchaeotal communities in mangrove wetlands suggests distinct niche preference of Bathyarchaeota subgroup 6. *Microb Ecol* 77:417–428. <https://doi.org/10.1007/s00248-018-1309-7>.
23. Stegen JC, Lin X, Konopka AE, Fredrickson JK. 2012. Stochastic and deterministic assembly processes in subsurface microbial communities. *ISME J* 6:1653–1664. <https://doi.org/10.1038/ismej.2012.22>.
24. Hanson CA, Fuhrman JA, Horner-Devine MC, Martiny JB. 2012. Beyond biogeographic patterns: processes shaping the microbial landscape. *Nat Rev Microbiol* 10:497–506. <https://doi.org/10.1038/nrmicro2795>.
25. Zhou JZ, Ning DL. 2017. Stochastic community assembly: does it matter in microbial ecology. *Microbiol Mol Biol Rev* 81:e00002-17. <https://doi.org/10.1128/MMBR.00002-17>.
26. Chen W, Ren K, Isabwe A, Chen H, Liu M, Yang J. 2019. Stochastic processes shape microeukaryotic community assembly in a subtropical river across wet and dry seasons. *Microbiome* 7:138. <https://doi.org/10.1186/s40168-019-0763-x>.
27. Pedrós-Alió C. 2012. The rare bacterial biosphere. *Annu Rev Mar Sci* 4:449–466. <https://doi.org/10.1146/annurev-marine-120710-100948>.
28. Lynch MD, Neufeld JD. 2015. Ecology and exploration of the rare biosphere. *Nat Rev Microbiol* 13:217–229. <https://doi.org/10.1038/nrmicro3400>.
29. Nuppenen-Puputti M, Purkamo L, Kietäväinen R, Nyyssönen M, Itävaara M, Ahonen L, Kukkonen I, Bomberg M. 2018. Rare biosphere archaea assimilate acetate in Precambrian terrestrial subsurface at 2.2 km depth. *Geosciences* 8:418. <https://doi.org/10.3390/geosciences8110418>.
30. Zhou L, Zhou Z, Lu Y-W, Ma L, Bai Y, Li X-X, Mbadanga SM, Liu Y-F, Yao X-C, Qiao Y-J, Zhang Z-R, Liu J-F, Yang S-Z, Wang W-D, Gu J-D, Mu B-Z. 2019. The newly proposed TACK and DPANN archaea detected in the production waters from a high-temperature petroleum reservoir. *Int Biodeterior Biodegradation* 143:104729. <https://doi.org/10.1016/j.ibiod.2019.104729>.
31. Yang S, Winkel M, Wagner D, Liebner S. 2017. Community structure of rare methanogenic archaea: insight from a single functional group. *FEMS Microbiol Ecol* 93:fix126. <https://doi.org/10.1093/femsec/fix126>.
32. Shade A, Jones SE, Caporaso JG, Handelsman J, Knight R, Fierer N, Gilbert JA. 2014. Conditionally rare taxa disproportionately contribute to temporal changes in microbial diversity. *mBio* 5:e01371-14. <https://doi.org/10.1128/mBio.01371-14>.
33. Liu X, Li M, Castelle CJ, Probst AJ, Zhou Z, Pan J, Liu Y, Banfield JF, Gu JD. 2018. Insights into the ecology, evolution, and metabolism of the widespread Woese archaeal lineages. *Microbiome* 6:102. <https://doi.org/10.1186/s40168-018-0488-2>.
34. Tedersoo L, Bahram M, Polme S, Koljalg U, Yorou NS, Wijesundera R, Villarreal Ruiz L, Vasco-Palacios AM, Thu PQ, Suija A, Smith ME, Sharp C, Saluveer E, Saitta A, Rosas M, Riit T, Ratkowsky D, Pritsch K, Poldmaa K, Piepenbring M, Phosri C, Peterson M, Parts K, Partel K, Otsing E, Nouhra E, Njouonkou AL, Nilsson RH, Morgado LN, Mayor J, May TW, Majuakim L, Lodge DJ, Lee SS, Larsson KH, Kohout P, Hosaka K, Hiiesalu I, Henkel TW, Harend H, Guo LD, Greslebin A, Grelet G, Geml J, Gates G, Dunstan W, Dunk C, Drenkhan R, Dearnaley J, De Kesel A, et al. 2014. Fungal biogeography. Global diversity and geography of soil fungi. *Science* 346:1256688. <https://doi.org/10.1126/science.1256688>.
35. Mendes LW, Taketani RG, Navarrete AA, Tsai SM. 2012. Shifts in phylogenetic diversity of archaeal communities in mangrove sediments at different sites and depths in southeastern Brazil. *Res Microbiol* 163:366–377. <https://doi.org/10.1016/j.resmic.2012.05.005>.
36. Li W, Guan W, Chen H, Liao B, Hu J, Peng C, Rui J, Tian J, Zhu D, He Y. 2016. Archaeal communities in the sediments of different mangrove stands at Dongzhaigang. *J Soils Sediments* 16:1995–2004. <https://doi.org/10.1007/s11368-016-1427-0>.
37. Imchen M, Kumavath R, Barh D, Vaz A, Goes-Neto A, Tiwari S, Ghosh P, Wattam AR, Azevedo V. 2018. Comparative mangrove metagenome reveals global prevalence of heavy metals and antibiotic resistome across different ecosystems. *Sci Rep* 8:11187. <https://doi.org/10.1038/s41598-018-29521-4>.
38. Yu T, Liang Q, Niu M, Wang F. 2017. High occurrence of Bathyarchaeota (MCG) in the deep-sea sediments of South China Sea quantified using newly designed PCR primers. *Environ Microbiol Rep* 9:374–382. <https://doi.org/10.1111/1758-2229.12539>.
39. Xiang X, Wang R, Wang H, Gong L, Man B, Xu Y. 2017. Distribution of Bathyarchaeota communities across different terrestrial settings and their potential ecological functions. *Sci Rep* 7:45028. <https://doi.org/10.1038/srep45028>.
40. Martín-Cuadrado AB, García-Heredia I, Molto AG, López-Ubeda R, Kimes N, López-García P, Moreira D, Rodríguez-Valera F. 2015. A new class of marine Euryarchaeota group II from the Mediterranean deep chlorophyll maximum. *ISME J* 9:1619–1634. <https://doi.org/10.1038/ismej.2014.249>.
41. Orsi WD, Smith JM, Wilcox HM, Swallow JE, Carini P, Worden AZ, Santoro AE. 2015. Ecophysiology of uncultivated marine euryarchaea is linked to particulate organic matter. *ISME J* 9:1747–1763. <https://doi.org/10.1038/ismej.2014.260>.
42. Orellana LH, Ben Francis T, Kruger K, Teeling H, Müller MC, Fuchs BM, Konstantinidis KT, Amann RL. 2019. Niche differentiation among annually recurrent coastal Marine Group II Euryarchaeota. *ISME J* 13:3024–3036. <https://doi.org/10.1038/s41396-019-0491-z>.
43. Rinke C, Rubino F, Messer LF, Youssef N, Parks DH, Chuvochina M, Brown M, Jeffries T, Tyson GW, Seymour JR, Hugenholtz P. 2019. A phylogenomic and ecological analysis of the globally abundant Marine Group II archaea (Ca. Poseidoniales ord. nov.). *ISME J* 13:663–675. <https://doi.org/10.1038/s41396-018-0282-y>.
44. Zhang X, Hu BX, Ren H, Zhang J. 2018. Composition and functional diversity of microbial community across a mangrove-inhabited mudflat as revealed by 16S rDNA gene sequences. *Sci Total Environ* 633:518–528. <https://doi.org/10.1016/j.scitotenv.2018.03.158>.
45. Dhal PK, Kopprio GA, Gardes A. 2020. Insights on aquatic microbiome of the Indian Sundarbans mangrove areas. *PLoS One* 15:e0221543. <https://doi.org/10.1371/journal.pone.0221543>.
46. Xiao J, Zhang Y, Chen W, Xu Y, Zhao R, Tao L, Wu Y, Zhang Y, Xiao X, Zhu R. 2020. Diversity and biogeography of Woese archaeota: a comprehensive analysis of multi-environment data. *bioRxiv* <https://doi.org/10.1101/2020.08.09.243345>.
47. Dini-Andreote F, Stegen JC, van Elsland JD, Salles JF. 2015. Disentangling mechanisms that mediate the balance between stochastic and deterministic processes in microbial succession. *Proc Natl Acad Sci U S A* 112:E1326–E1332. <https://doi.org/10.1073/pnas.1414261112>.
48. Jiao S, Lu Y. 2020. Soil pH and temperature regulate assembly processes of abundant and rare bacterial communities in agricultural ecosystems. *Environ Microbiol* 22:1052–1065. <https://doi.org/10.1111/1462-2920.14815>.
49. Morlon H, Chuyong G, Condit R, Hubbell S, Kenfack D, Thomas D, Valencia R, Green JL. 2008. A general framework for the distance-decay of similarity in ecological communities. *Ecol Lett* 11:904–917. <https://doi.org/10.1111/j.1461-0248.2008.01202.x>.
50. Bahram M, Kohout P, Anslan S, Harend H, Abarenkov K, Tedersoo L. 2016. Stochastic distribution of small soil eukaryotes resulting from high dispersal and drift in a local environment. *ISME J* 10:885–896. <https://doi.org/10.1038/ismej.2015.164>.
51. Liu L, Yang J, Yu Z, Wilkinson DM. 2015. The biogeography of abundant and rare bacterioplankton in the lakes and reservoirs of China. *ISME J* 9:2068–2077. <https://doi.org/10.1038/ismej.2015.29>.
52. Wu W, Logares R, Huang B, Hsieh CH. 2017. Abundant and rare picoeukaryotic sub-communities present contrasting patterns in the epipelagic waters of marginal seas in the northwestern Pacific Ocean. *Environ Microbiol* 19:287–300. <https://doi.org/10.1111/1462-2920.13606>.
53. Jiao S, Lu Y. 2020. Abundant fungi adapt to broader environmental gradients than rare fungi in agricultural fields. *Glob Chang Biol* 26:4506–4520. <https://doi.org/10.1111/gcb.15130>.

54. Pandit SN, Kolasa J, Cottenie K. 2009. Contrasts between habitat generalists and specialists an empirical extension to the basic metacommunity framework. *Ecology* 90:2253–2262. <https://doi.org/10.1890/08-0851.1>.
55. Jiao S, Chen W, Wei G. 2017. Biogeography and ecological diversity patterns of rare and abundant bacteria in oil-contaminated soils. *Mol Ecol* 26:5305–5317. <https://doi.org/10.1111/mec.14218>.
56. Mo Y, Zhang W, Yang J, Lin Y, Yu Z, Lin S. 2018. Biogeographic patterns of abundant and rare bacterioplankton in three subtropical bays resulting from selective and neutral processes. *ISME J* 12:2198–2210. <https://doi.org/10.1038/s41396-018-0153-6>.
57. Zhang ZF, Cai L. 2019. Substrate and spatial variables are major determinants of fungal community in karst caves in Southwest China. *J Biogeogr* 46:1504–1518. <https://doi.org/10.1111/jbi.13594>.
58. Logares R, Lindström ES, Langenheder S, Logue JB, Paterson H, Laybourn-Parry J, Rengefors K, Tranvik L, Bertilsson S. 2013. Biogeography of bacterial communities exposed to progressive long-term environmental change. *ISME J* 7:937–948. <https://doi.org/10.1038/ismej.2012.168>.
59. Zhang W, Pan Y, Yang J, Chen H, Holohan B, Vaudrey J, Lin S, McManus GB. 2018. The diversity and biogeography of abundant and rare intertidal marine microeukaryotes explained by environment and dispersal limitation. *Environ Microbiol* 20:462–476. <https://doi.org/10.1111/1462-2920.13916>.
60. Zhang ZF, Pan YP, Liu Y, Li M. 2020. Pacific Biosciences single-molecule real-time (SMRT) sequencing reveals high diversity of basal fungal lineages and stochastic processes controlled fungal community assembly in mangrove sediments. *ResearchSquare* <https://doi.org/10.21203/rs.3.rs-93764/v1>.
61. Lima-Mendez G, Faust K, Henry N, Decelle J, Colin S, Carcillo F, Chaffron S, Ignacio-Espinosa JC, Roux S, Vincent F, Bittner L, Darzi Y, Wang J, Audic S, Berline L, Bontempi G, Cabello AM, Coppola L, Cornejo-Castillo FM, d'Ovidio F, De Meester L, Ferrera I, Garet-Delmas M-J, Guidi L, Lara E, Pesant S, Royo-Llonch M, Salazar G, Sánchez P, Sebastian M, Souffreau C, Dimier C, Picheral M, Searson S, Kandels-Lewis S, Tara Oceans coordinators, Gorsky G, Not F, Ogata H, Speich S, Stemmann L, Weissenbach J, Wincker P, Acinas SG, Sunagawa S, Bork P, Sullivan MB, Karsenti E, Bowler C, de Vargas C, Raes J. 2015. Determinants of community structure in the global plankton interactome. *Science* 348:1262073. <https://doi.org/10.1126/science.1262073>.
62. Wei G, Li M, Li F, Li H, Gao Z. 2016. Distinct distribution patterns of prokaryotes between sediment and water in the Yellow River estuary. *Appl Microbiol Biotechnol* 100:9683–9697. <https://doi.org/10.1007/s00253-016-7802-3>.
63. Banerjee S, Walder F, Buchi L, Meyer M, Held AY, Gattinger A, Keller T, Charles R, van der Heijden MGA. 2019. Agricultural intensification reduces microbial network complexity and the abundance of keystone taxa in roots. *ISME J* 13:1722–1736. <https://doi.org/10.1038/s41396-019-0383-2>.
64. Berry D, Widder S. 2014. Deciphering microbial interactions and detecting keystone species with co-occurrence networks. *Front Microbiol* 5:219. <https://doi.org/10.3389/fmicb.2014.00219>.
65. Faust K, Raes J. 2012. Microbial interactions: from networks to models. *Nat Rev Microbiol* 10:538–550. <https://doi.org/10.1038/nrmicro2832>.
66. Shi Y, Fan K, Li Y, Yang T, He JS, Chu H. 2019. Archaea enhance the robustness of microbial co-occurrence networks in Tibetan Plateau soils. *Soil Sci Soc Am J* 83:1093–1099. <https://doi.org/10.2136/sssaj2018.11.0426>.
67. Faust K, Lima-Mendez G, Lerat JS, Sathirapongsasuti JF, Knight R, Huttenhower C, Lenaerts T, Raes J. 2015. Cross-biome comparison of microbial association networks. *Front Microbiol* 6:1200. <https://doi.org/10.3389/fmicb.2015.01200>.
68. Chouari R, Guermazi S, Sghir A. 2015. Co-occurrence of Crenarchaeota, Thermoplasmata and methanogens in anaerobic sludge digesters. *World J Microbiol Biotechnol* 31:805–812. <https://doi.org/10.1007/s11274-015-1834-1>.
69. Zhou Z, Pan J, Wang F, Gu JD, Li M. 2018. Bathyarchaeota: globally distributed metabolic generalists in anoxic environments. *FEMS Microbiol Rev* 42:639–655. <https://doi.org/10.1093/femsre/fuy023>.
70. Baker BJ, De Anda V, Seitz KW, Dombrowski N, Santoro AE, Lloyd KG. 2020. Diversity, ecology and evolution of Archaea. *Nat Microbiol* 5:887–900. <https://doi.org/10.1038/s41564-020-0715-z>.
71. Lavergne C, Hugoni M, Dupuy C, Agogue H. 2018. First evidence of the presence and activity of archaeal C3 group members in an Atlantic intertidal mudflat. *Sci Rep* 8:11790. <https://doi.org/10.1038/s41598-018-30222-1>.
72. Coolen MJL, Hopmans EC, Rijpstra WIC, Muyzer G, Schouten S, Volkman JK, Sinninghe Damsté JS. 2004. Evolution of the methane cycle in Ace Lake (Antarctica) during the Holocene: response of methanogens and methanotrophs to environmental change. *Org Geochem* 35:1151–1167. <https://doi.org/10.1016/j.orggeochem.2004.06.009>.
73. Cheng YF, Mao SY, Liu JX, Zhu WY. 2009. Molecular diversity analysis of rumen methanogenic Archaea from goat in eastern China by DGGE methods using different primer pairs. *Lett Appl Microbiol* 48:585–592. <https://doi.org/10.1111/j.1472-765X.2009.02583.x>.
74. Joshi NA, Fass JN. 2011. Sickle: a sliding-window, adaptive, quality-based trimming tool for FastQ files, v1.33. <https://github.com/najoshi/sickle>.
75. Edgar RC. 2010. Search and clustering orders of magnitude faster than BLAST. *Bioinformatics* 26:2460–2461. <https://doi.org/10.1093/bioinformatics/btq461>.
76. Edgar RC. 2013. UPARSE: highly accurate OTU sequences from microbial amplicon reads. *Nat Methods* 10:996–998. <https://doi.org/10.1038/nmeth.2604>.
77. Quast C, Pruesse E, Yilmaz P, Gerken J, Schweer T, Yarza P, Peplies J, Glockner FO. 2013. The SILVA ribosomal RNA gene database project: improved data processing and web-based tools. *Nucleic Acids Res* 41:D590–D596. <https://doi.org/10.1093/nar/gks1219>.
78. Camacho C, Coulouris G, Avagyan V, Ma N, Papadopoulos J, Bealer K, Madden TL. 2009. BLAST+: architecture and applications. *BMC Bioinformatics* 10:421. <https://doi.org/10.1186/1471-2105-10-421>.
79. Paulson JN, Stine OC, Bravo HC, Pop M. 2013. Differential abundance analysis for microbial marker-gene surveys. *Nat Methods* 10:1200–1202. <https://doi.org/10.1038/nmeth.2658>.
80. Jonsson V, Osterlund T, Neran O, Kristiansson E. 2016. Statistical evaluation of methods for identification of differentially abundant genes in comparative metagenomics. *BMC Genomics* 17:78. <https://doi.org/10.1186/s12864-016-2386-y>.
81. Paulson JN, Olson ND, Braccia DJ, Wagner J, Talukder H, Pop M, Bravo HC. 2013. metagenomeSeq: statistical analysis for sparse high-throughput sequencing. *Bioconductor package*, <http://www.cbc.umd.edu/software/metagenomeSeq>.
82. Oksanen J, Blanchet FG, Friendly M, Kindt R, Legendre P, D M, Minchin PR, O'Hara RB, Simpson GL, Solymos P, Stevens MHH, Szoecs E, Wagner H. 2019. vegan: Community Ecology Package. R package version 2.5–6., <https://CRAN.R-project.org/package=vegan>.
83. Li W, Wang M, Pan H, Burgaud G, Liang S, Guo J, Luo T, Li Z, Zhang S, Cai L. 2018. Highlighting patterns of fungal diversity and composition shaped by ocean currents using the East China Sea as a model. *Mol Ecol* 27:564–576. <https://doi.org/10.1111/mec.14440>.
84. Sloan WT, Lunn M, Woodcock S, Head IM, Nee S, Curtis TP. 2006. Quantifying the roles of immigration and chance in shaping prokaryote community structure. *Environ Microbiol* 8:732–740. <https://doi.org/10.1111/j.1462-2920.2005.00956.x>.
85. Wang Y, Pan J, Yang J, Zhou Z, Pan Y, Li M. 2020. Patterns and processes of free-living and particle-associated bacterioplankton and archaeoplankton communities in a subtropical river-bay system in South China. *Limnol Oceanogr* 65:S161–S179. <https://doi.org/10.1002/lno.11314>.
86. Burns AR, Stephens WZ, Stagaman K, Wong S, Rawls JF, Guillemin K, Bohannan BJ. 2016. Contribution of neutral processes to the assembly of gut microbial communities in the zebrafish over host development. *ISME J* 10:655–664. <https://doi.org/10.1038/ismej.2015.142>.
87. Hijmans RJ. 2019. geosphere: spherical trigonometry. R package version 1.5–10. <https://CRAN.R-project.org/package=geosphere>.
88. Tripathi BM, Stegen JC, Kim M, Dong K, Adams JM, Lee YK. 2018. Soil pH mediates the balance between stochastic and deterministic assembly of bacteria. *ISME J* 12:1072–1083. <https://doi.org/10.1038/s41396-018-0082-4>.
89. Legendre P, Gallagher ED. 2001. Ecologically meaningful transformations for ordination of species data. *Oecologia* 129:271–280. <https://doi.org/10.1007/s004420100716>.
90. Reshef DN, Reshef YA, Finucane HK, Grossman SR, McVean G, Turnbaugh PJ, Lander ES, Mitzenmacher M, Sabeti PC. 2011. Detecting novel associations in large data sets. *Science* 334:1518–1524. <https://doi.org/10.1126/science.1205438>.
91. Weiss S, Van Treuren W, Lozupone C, Faust K, Friedman J, Deng Y, Xia LC, Xu ZZ, Ursell L, Alm EJ, Birmingham A, Cram JA, Fuhrman JA, Raes J, Sun F, Zhou J, Knight R. 2016. Correlation detection strategies in microbial data sets vary widely in sensitivity and precision. *ISME J* 10:1669–1681. <https://doi.org/10.1038/ismej.2015.235>.
92. Albanese D, Riccadonna S, Donati C, Franceschi P. 2018. A practical tool for maximal information coefficient analysis. *Gigascience* 7:1–8. <https://doi.org/10.1093/gigascience/giy032>.
93. Peura S, Bertilsson S, Jones RI, Eiler A. 2015. Resistant microbial co-occurrence patterns inferred by network topology. *Appl Environ Microbiol* 81:2090–2097. <https://doi.org/10.1128/AEM.03660-14>.
94. Csardi G, Nepusz T. 2006. The igraph software package for complex network research. *InterJournal, Complex Systems* 1695:1–9.

95. Bastian M, Heymann S, Jacomy M. 2009. Gephi: an open source software for exploring and manipulating networks, p 361–362. *In Proc Third Int ICWSM Conf.* AAAI Press, Menlo Park, CA.
96. Zhu HZ, Zhang ZF, Zhou N, Jiang CY, Wang BJ, Cai L, Liu SJ. 2019. Diversity, distribution and co-occurrence patterns of bacterial communities in a karst cave system. *Front Microbiol* 10:1726. <https://doi.org/10.3389/fmicb.2019.01726>.
97. Cheung MK, Wong CK, Chu KH, Kwan HS. 2018. Community structure, dynamics and interactions of bacteria, archaea and fungi in subtropical coastal wetland sediments. *Sci Rep* 8:14397. <https://doi.org/10.1038/s41598-018-32529-5>.
98. Banerjee S, Schlaeppi K, van der Heijden MGA. 2018. Keystone taxa as drivers of microbiome structure and functioning. *Nat Rev Microbiol* 16:567–576. <https://doi.org/10.1038/s41579-018-0024-1>.